Climate impact of Norwegian emissions of short-lived climate forcers

Report written by Center for International Climate and Environmental Research – Oslo (CICERO) on commission from The Norwegian Environment Agency

Version:

19 September, 2014

Øivind Hodnebrog, Borgar Aamaas, Terje K. Berntsen, Jan S. Fuglestvedt, Gunnar Myhre, Bjørn H. Samset, Amund Søvde

Table of Contents

1. Summary

This report presents the global climate impact for emissions in Norway of various gases and particles: CH_4, HFCs, BC, OC, SO_2 and the ozone precursors NO_x, CO and nmVOC. The climate impact is given in terms of different emission metrics. The two most common emission metrics are "Global Warming Potential" (GWP) and "Global Temperature change Potential" (GTP). GWP is based on integrated radiative forcing and GTP on global mean surface temperature change. In addition, we present regional emission metrics based on temperature change in different latitude bands for emissions of ozone precursors (NO_x, CO and nmVOC), aerosol precursors (SO_2) and aerosols (BC and OC). This regional emission metric is called "Absolute Regional Temperature change Potential" (ARTP). We also present near-surface ozone concentrations that can be attributed to emissions in Norway. The emission metrics calculated for emissions in Norway are similar to emission metrics for global emissions, but with some exceptions. For instance, the direct effect of aerosols (absorption/reflection of incoming solar radiation in the atmosphere) is weaker for Norwegian emissions than for global emissions, while at the same time the albedo effect on snow and ice from BC (change in reflection) is much stronger. The regional emission metrics are based on new and limited research; hence, caution should be used when interpreting the regional emission metrics presented here.

The work is done on commission of the Norwegian Environment Agency.

2. Introduction

The Norwegian Environment Agency made a call in 2012 for a project that should give information on the climate impact of emissions of short-lived climate forcers in Norway. The results will be applied in the Norwegian Environment Agency's work to make an action plan to reduce Norwegian emissions of short-lived climate forcers. "Short-lived climate forcers" are here understood as ozone, black carbon (BC), methane (CH_4), and all nine HFC gases that are emitted in Norway (HFC-23, HFC-32, HFC-125, HFC-134, HFC-134a, HFC-143, HFC-143a, HFC-152a, and HFC-227ea). The climate impacts of SO_2 and OC have also been modelled as the components lead to cooling and are often co-emitted with some of the short-lived climate forcers.

In connection to the action plan, CICERO has also evaluated different methods to estimate the climate impact of different short-lived climate forcers and long-lived greenhouse gases with focus on the usage of different emission metrics, such as GWP and GTP (Aamaas et al., 2012).

GWP is based on integrated radiative forcing, where radiative forcing is the change in energy per surface area for the world measured at the top of the atmosphere (see glossary for complete definition). GTP is defined from a change in global surface temperature. For a broader introduction to the usage of emission metrics, see Aamaas et al. (2013). We here define nmVOC as volatile organic compounds with the exception of CH_4.

The climate impact of these gases and particles has been calculated for Norwegian emissions specifically, except for CH_4 and HFCs, in which we use existing literature (see Section 3.4.1) since the climate impact is less dependent on emission location for gases with a lifetime of more than a few months. Limitations and methods used are given in Section 3, while Section 4 shows the results presented in tables that give GWP and GTP values for a range of time horizons (see also Annex 1,

Excel sheet "GWP_GTP_pulse_scenario_ENGLISH.xlsx") as well as CO_2 equivalent emissions for the ozone precursors and aerosols. No matter what emission metric and time horizon is applied, the emissions are calculated into CO_2 equivalent emissions since the reference gas is CO_2. However, the emissions are only CO_2 equivalent for the specific emission metric and time horizon chosen. Hence, GWP with a time horizon of 100 years is not the only emission metric that give emissions in CO_2 equivalents. For other emission metrics and time horizons, one can also give emissions in CO_2 equivalents, but the weighing of the various gases and particles will differ. The emission metrics are given for two types of emission profiles. The standard method is to calculate emission metrics for a pulse emission, in which all emissions occur in the first year followed by no emissions. The other type is an emission metric that is based on a gradual implementation of a mitigation policy from 2010 to 2020, followed by constant change in emissions. The Norwegian Environment Agency wanted to include the latter type of emission metric because such an emission profile is in line with what is expected due to commitments in the Gothenburg Protocol, as well as a check on the robustness of the climate impact of reducing emissions of NO_X.

3. Methods

3.1. Definition of regions

The Norwegian emissions have been split into four regions in agreement with the Norwegian Environment Agency. Figure 1 shows emissions of NO_X in each of the regions that are shortly described here:

1. **East:** Emissions from land south of 63°N and east of 8°E.
2. **West:** Emissions from land south of 63°N and west of 8°E.
3. **North:** Emissions from land north of 63°N.
4. **Offshore:** All emissions from national shipping activity and emissions outside of the Norwegian coastline. To implement the emissions outside of the coastline in the best manner, a 2-dimensional data field was created to give information, for each grid cell, whether the underlying surface were primarily land or ocean. Emissions over land were then assigned to one of the three land regions, while emissions over ocean and emissions in the category "national shipping", were assigned to the "offshore" region.

This separation between regions is due to the natural separation between east and west, as well as north versus the rest of the country. Since the emissions are low or non-existent in Langfjella and Dovrefjell, the borders between the regions were set in these mountain regions. In addition, emissions from offshore are natural to separate out since the emissions can have a different mix, as well as the emissions occur over ocean and will, thus, possibly give other climate impacts than emissions over land. A further division of smaller regions was not appropriate due the limitations of the project, the resolution of the model we applied, and that every region must have significant emissions (to minimize numerical noise due to rounding errors – see Section 3.2) to model a climate impact.

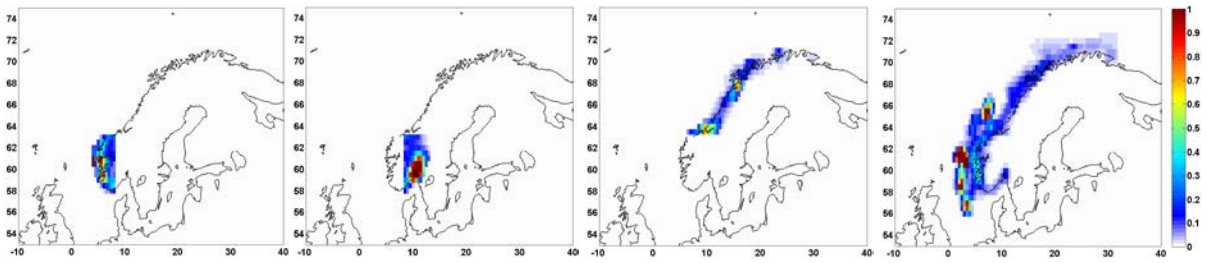

Figure 1. Gridded emissions of NO_X (given as kt (NO_2)/year) for 2010 in each of the regions west, east, north, and offshore.

3.2. Emissions and implementation

Norwegian emissions of CO, NO_X, nmVOC, SO_2, and PM2.5 from 2010 were provided by the Norwegian Environment Agency and implemented in the chemical transport model applied here (see Section 3.3). The objective of this report is to estimate emission metrics, i.e., climate impacts **per unit of emission**. Hence, the small differences between the original emission dataset (delivered by the Norwegian Environment Agency) and the emissions applied in the model here (see below) are likely to have negligible impact on the results presented here.

Since the model depends on emissions of BC and OC, the Norwegian Environment Agency has delivered factors to convert emissions of PM2.5 into BC and OC for each emission sector. Similarly, the total emissions of nmVOCs (hydrocarbons) were divided into different nmVOC species following methods previously applied in the EU project ECLIPSE. Since we estimate the global response, and therefore use global models, we also need data on the distribution of global emissions. For regions outside of Norway, we have applied anthropogenic emissions delivered by IIASA. These emissions are accessible through ECLIPSE[1]. Emissions for international air and ship traffic come from the RCP6.0 pathway (Fujino et al., 2006; van Vuuren et al., 2011), while emissions from biomass burning are taken from Global Fire Emissions Database (GFED) version 3 (van der Werf et al., 2010). All the anthropogenic emissions, both Norwegian and global, are for the year 2010, while the emissions from biomass burning are from the same years as the meteorological data (2006 and 2007) and are updated every month.

The original anthropogenic emission dataset contain annual total emissions per sector, thus, without any monthly variations. In reality, the emissions will vary over the year, especially due to increased heating demand by households during winter (e.g., Streets et al., 2003). This seasonal variation has been taken into consideration by applying a method described in Section 3.3 in Streets et al. (2003). The emissions in the domestic sector are implemented in the chemical transport model with a monthly variation based on the outdoor temperature, for instance the emissions of CO are greater in winter due to increased heating demand by households. This assumption is rather crude since other emission sectors than “domestic” also have some variation with season; however, good information

[1] Emission data are available upon request – see http://eclipse.nilu.no/.

on seasonal variations of anthropogenic emissions are generally lacking (Streets et al., 2003). The temperature fields applied for this adjustment come from Climatic Research Unit[2] (CRU) and are an average over the seven years 2000-2006. The following assumption between heating and temperature was used: <0°C, 16 hours/day; 0-5°C, 12 hours/day; 5-10°C, 6 hours/day; >10°C, 3 hours/day (Streets et al., 2003). Table 1 shows the emissions separated according to component, season, and region. The table shows, for instance, that Eastern Norway has the largest emissions of CO and nmVOC, while the emissions of NO_x are greatest in the offshore region. Note that the emissions given in Table 1 deviate somewhat from the national emissions provided by the Norwegian Environment Agency, and this is mainly due to technicalities. More specifically, emissions from the fishing fleet south of 55°N and west of 0° are not included in the offshore region, and national emissions from landing/take-off (LTO) for air traffic are not included in the land regions. The latter was done to avoid double counting as we assume the national LTO emissions are part of the RCP dataset. In addition, the emissions had to be interpolated to the same grid as the global ECLIPSE dataset, and some small adjustments along the country borders (mainly Sweden) were applied to avoid overlapping with the ECLIPSE emissions. For BC and OC, the concentration is close to linearly increasing with increasing emissions; hence, the size of the emissions is of little importance – the most important factor is where the emissions occurred. The ozone chemistry is more non-linear and the size of the emissions of the ozone precursors are therefore more important for the ozone concentrations, and thus also for the climate impact. The official 2010 emissions from Norway (as reported in 2013) were 336.7 kt (CO), 185.2 kt (NO_2), 141.9 kt (nmVOC) and 19.4 kt (SO_2). The very first Norwegian emission inventories for BC and OC were published in spring 2013 and show that the emissions in 2010 were 5.6 kt (BC) and 22.5 kt (OC). In comparison to the Norwegian emissions used in the model, given in Table 1, the total **global** anthropogenic emissions from ECLIPSE for 2010 are 540 Mt[3](CO), 88 Mt(NO_2), 110 Mt(nmVOC), 92 Mt(SO_2), 5.5 Mt(BC) and 12 Mt(OC) for CO, NO_X, nmVOC, SO_2, BC and OC, respectively (emissions from biomass burning and international shipping and aviation are not included in these estimates).

[2] See http://badc.nerc.ac.uk/view/badc.nerc.ac.uk__ATOM__dataent_1256223773328276 for more information.

[3] Mt=10^6 ton =Tg=10^{12} gram. Kilo ton (kt)=10^3 ton= Gg

Table 1. Emissions of gases and particles in different regions in Norway and for different seasons in 2010. The unit is kiloton (kt), whereas NO_x is given as kt NO_2. All data on national emissions, including necessary factors to convert from PM2.5 to BC and OC, have been delivered by the Norwegian Environment Agency.

	CO				
	Winter	Spring	Summer	Autumn	Annual
East	54.4	45.5	29.3	39.2	168.4
West	21.9	19.1	12.9	15.8	69.8
North	18.8	17.0	10.7	14.5	60.9
Offshore	3.7	3.7	3.7	3.7	14.9
Total	98.8	85.4	56.7	73.1	313.9
	NO_x				
	Winter	Spring	Summer	Autumn	Annual
East	9.3	9.3	9.0	9.1	36.9
West	6.1	6.1	6.0	6.0	24.2
North	5.6	5.7	5.6	5.6	22.4
Offshore	22.4	22.9	22.9	22.7	90.9
Total	43.4	44.1	43.6	43.4	174.5
	nmVOC				
	Winter	Spring	Summer	Autumn	Annual
East	15.9	15.5	14.4	15.0	60.8
West	11.4	11.4	11.0	11.1	44.9
North	5.3	5.3	4.8	5.0	20.4
Offshore	2.9	2.9	2.9	2.9	11.6
Total	35.4	35.1	33.1	34.0	137.6
	SO_2				
	Winter	Spring	Summer	Autumn	Annual
East	1.27	1.25	1.16	1.20	4.88
West	0.98	0.97	0.92	0.94	3.81
North	1.41	1.43	1.40	1.40	5.64
Offshore	0.84	0.86	0.86	0.85	3.40
Total	4.50	4.50	4.34	4.39	17.73
	BC				
	Winter	Spring	Summer	Autumn	Annual
East	0.75	0.66	0.49	0.59	2.49
West	0.42	0.40	0.33	0.36	1.51
North	0.49	0.47	0.40	0.44	1.80
Offshore	0.33	0.33	0.33	0.33	1.32
Total	1.98	1.86	1.56	1.72	7.12
	OC				
	Winter	Spring	Summer	Autumn	Annual
East	3.84	2.83	1.08	2.17	9.92
West	1.54	1.22	0.56	0.88	4.20
North	1.51	1.30	0.61	1.03	4.46
Offshore	0.21	0.21	0.21	0.21	0.84
Total	7.10	5.57	2.46	4.29	19.43

The model calculations have been carried out with the same method commonly applied for this kind of studies – where the climate impact of emissions is quantified with a chemical transport model. This method starts with a reference simulation (for example called REF), where all emissions are included in the model and one tries often to simulate the atmospheric conditions close to the reality. Afterwards, one or more perturbation runs (for example called PERT) are produced, in which the

emissions are reduced or increased (hence, perturbed) for a chosen region or emission sector, for a given gas or aerosol, and over some time period. In the analysis, one wants to compare the results from the reference simulation with the perturbation simulation by looking at the difference between these two, for instance REF minus PERT (or PERT minus REF, depending on if the emission perturbation is an increase or a decrease relative to the reference). In this study, an example of a perturbation simulation is a 20% reduction of BC emissions in Eastern Norway for the summer season. If one wants to quantify the radiative forcing (RF) for all BC emissions in Eastern Norway in the summer season, one can after the simulations are finished, given that the system is close to linear, scale the results with a factor, *f*:

$$RF_{BC,East} = f*(RF_{REF}-RF_{PERT,BC,East,-20\%}).$$

In this case, *f*=5 will give the response of a 100% perturbation of emissions (5*20% = 100%). When we calculate the emission metrics, we are interested in the normalized radiative forcing, hence, RF per kg of emissions. This quantity can be calculated by selecting a *f* that equals 1 divided by the amount of emissions (in kg) for what was perturbed. For this example, $f = 1/(20\%*0.49x10^6$ kg(BC)) will give *RF* for 1 kg of BC emissions in Eastern Norway during the summer season.

For BC and OC, we used in our model calculations a 20% perturbation of emissions in each region and normalization to 1 kg of emissions, as the example above for BC in Eastern Norway. For the other components, where the non-linearities are more important than for BC and OC, a 20% perturbation proved to be too small. Since numerical models have limited accuracy, rounding errors will occur and could in some cases grow in proportion to give numerical noise in the results. Such issues are normally not a problem in atmospheric chemistry modelling since the emission perturbations are normally relatively large, but we encountered this issue when the emission perturbations are relatively small. In order to minimize contributions from non-linearities in the chemistry and numerical noise, we have chosen to multiply the emissions of CO with 10 (thus, an increase of 900%), NO_X with 2, nmVOC with 5, SO_2 with 2, BC with 0.8 (hence a reduction of 20%) and OC with 0.8, for each region and season. Normalized radiative forcings were afterwards calculated for each case, as the effect of 1 kg of emissions from each region and season.

3.3. Model tools and setup

A global chemistry transport model, Oslo CTM2 (Søvde et al., 2008), was used to estimate changes in atmospheric concentrations due to changes in Norwegian emissions of CO, NO_X, nmVOC, SO_2, BC and OC. This model has been developed and utilized over many years at the Department of Geosciences at the University of Oslo, and Center for International Climate and Environmental Research – Oslo (CICERO) (e.g., Berglen et al., 2004; Berntsen et al., 2006; Skeie et al., 2011). For the calculations of ozone chemistry and sulphates, the model has been run with modules for tropospheric chemistry (Berntsen and Isaksen, 1997), sulphur (Berglen et al., 2004), nitrate (Myhre et al., 2006) and sea salt (Grini et al., 2002), while calculations of BC/OC have been executed separately in an own module (Berntsen et al., 2006). As opposed to climate models, a chemical transport model is normally driven by analysed, i.e. "real," meteorological fields, in this case from ECMWF (European Centre for Medium-Range Weather Forecasts), hence, changes in concentration of gases and particles will

therefore have no impact on the meteorology. From this follows that we can only calculate the direct aerosol effect (as well as the albedo effect of BC on snow and ice) here, while the indirect aerosol effects will be discussed in the section on uncertainties (Section 4.2.3). A large and decisive advantage of using Oslo CTM2 is that detailed calculations of chemistry and transport of gases and particles are included. Until recently, calculations of gas phase and aerosol chemistry was often very simplified in global climate models.

The model has been run with meteorological data for both 2006 and 2007 to reduce the results' dependency on choice of meteorological year. These years are complementary, as 2006 was mild and with precipitation close to the normal (1961-1990), while 2007 was a bit cooler and with more precipitation than normal. 2007 was in particular wet during the spring and winter, as opposed to 2006 that had a dry spring and summer, but somewhat wetter autumn. The spring was extra cold in 2006, while mild in 2007. If not otherwise stated, the results presented in this report are given as the average of 2006 and 2007. The resolution horizontally is T42, i.e. grids covering about 2.8° longitude and 2.8° latitude, and 60 layers vertically. The thickness of the vertical layers varies with height, and they are thinnest near the ground – the lowest vertical layer has a thickness of about 16 meters.

For the ozone precursors, the ozone concentrations calculated from the Oslo CTM2 model have been applied in a radiative transfer model (Myhre et al., 2000) to estimate the radiative forcing from changes in ozone concentrations. The horizontal resolution in the radiative transfer model is T21 (about 5.6° longitude and 5.6° latitude), while the vertical resolution is the same as in Oslo CTM2 (60 layers).

Emissions of ozone precursors also impact the concentration of OH, which further impact the lifetime of the greenhouse gas methane. The method applied to calculate the radiative forcing from changes in methane is explained by Berntsen et al. (2005) and implies first to multiply the change in the lifetime of methane with the assumed methane concentration from IPCC (2001). A factor of 1.4 has been applied to consider the effect of changes in methane on its own lifetime (IPCC, 2001). Further, we have assumed a normalized radiative forcing for methane of 0.37 mW m^{-2} ppb^{-1} (Forster et al., 2007) for an assumed background concentration of 1740 ppb. Finally, we have included the effect on changes in methane on stratospheric water vapour by multiplying the radiative forcing of the changes in methane with a factor of 1.15 (Myhre et al., 2007b). Since methane is also an ozone precursor, the changes in the lifetime of the methane will also affect the radiative forcing of ozone, and this effect is considered by assuming an increase in ozone of 0.64 DU for a 10% increase in methane (Berntsen et al., 2005) and a normalized radiative forcing for ozone of 42 mW m^{-2} DU^{-1} (IPCC, 2001). In summary, these effects are accounted for in the calculations:

- Ozone is not emitted directly, but is formed photochemically by the precursors CO, NOx, and nmVOC (hydrocarbons) → Warming effect
- Emissions of NO_x will in addition increase the amount of OH, which leads to a reduction of methane (CH_4) → Cooling effect
- Emissions of CO and nmVOC reduce the amount of OH, which leads to an increase of methane (CH_4) → Warming effect
- The increase (the decrease) of methane (CH_4) will further lead to an increase (decrease) in ozone → Warming (cooling). This effect is often called the ozone "primary mode" and occurs

on a longer time scale than the photochemical formation of ozone from CO, NO_X and nmVOC (described in the first point).

For the aerosol, the concentrations estimated with Oslo CTM2 have been weighed with normalized radiative forcings for BC, OC, and sulphate in every single grid box. Normalized radiative forcings are changes in radiative forcings given per change in concentration, in this case as W g^{-1} for each grid box, and when these values are multiplied with concentrations, we find the radiative forcing in W m^{-2}. The normalized radiative forcings have been estimated beforehand with detailed radiation models (Myhre et al., 2007a) run with a T42 horizontal resolution (2.8° × 2.8°) and 3 hour time step. Samset and Myhre (2011) show the normalized radiation forcings for BC and sulphate, and we have applied same method for OC.

3.4. Emission metrics

3.4.1. Global emission metrics

The emission metrics GWP and GTP have been calculated for the various gases and particles in different regions, in the same manner as described in Aamaas et al. (2012; 2013) and Fuglestvedt et al. (2010). The calculations are based on estimated radiative forcing per kg of emissions, atmospheric lifetime of the gases and particles, as well as a global temperature response from the radiative forcing for the GTP. For the greenhouse gases methane and HFCs, the emission metrics presented here are identical to the values in the Fourth Assessment Report from the IPCC (Forster et al., 2007). In addition, we also include emission metric values from a large study by Hodnebrog et al. (2013) for the HFCs. Values for GWP and GTP have been calculated with two different time profiles of emissions, 1) pulse emissions and 2) a gradual ramp up of mitigation measures from 2010 to 2020, followed by a constant level.

For the calculations for the pulse emissions, we estimate the effect over time of emissions that occur during the first year, which is the standard setup for calculations of GWP and GTP values. Emission metrics based on pulse emissions are applicable and flexible, and the responses of pulses from different years can be combined to a scenario by the use of convolutions (Berntsen and Fuglestvedt, 2008; Aamaas et al., 2012; Aamaas et al., 2013). Convolution is a mathematical operation on two functions to make a third function that is a modified version of one of the original functions. The second type of time profile for emissions was applied because the Norwegian Environment Agency wanted to include emission metrics based on an emission profile in accordance with what to be expected from the commitments under the Gothenburg Protocol, as well as give insight on how robust the results are, especially on the climate impact of reducing NO_x. This scenario has been calculated by using pulse values and convolution as described above. We have assumed that the mitigation measure is gradually implemented, with a linear increase in emission cut throughout the introduction period. In practice, the first 9% of the cut is taken in 2010 and the last 9% in 2020. If the total mitigation measure leads to an emission reduction of 1 kg/year in 2020, then the emission reduction in the years between 2010 and 2020 in kg/year in year *t* will be:

$$E(t) = \frac{t - 2009}{11}$$

All these GWP and GTP values are given for a change in emissions of 1 kg relative to the same change for the reference gas CO_2 (Forster et al., 2007; Fuglestvedt et al., 2010). These values can easily be converted into the climate impact of the expected emission cut. The recalculation is achieved by multiplying the change in emissions with the emission metric for the gas or particle in question. For instance, the expected cut in Norwegian emissions of nmVOC from 2010 to 2020 is 142 – 131 kt = 11 kt, which has to be multiplied with the emission metric. This calculation gives the CO_2 equivalent emissions in kt for a change in emissions of CO_2 following the same emission pathway that gives the same climate impact for the chosen emission metric and time horizon. However, the emissions are only CO_2 equivalent for this specific emission metric and time horizon.

The emission metrics for the gradual ramp up of mitigation measures are not shown in the report, but are available in Annex 1 (see the Excel sheet «GWP_GTP_pulse_scenario_ENGLISH.xlsx»). Since this emission profile is similar to a profile with sustained emissions, the climate impact of species with a shorter perturbation lifetime of the atmosphere than CO_2 will have a somewhat higher emission metric for a span of time horizons. The short-lived climate forcers will be "forgotten" after some time in the climate system for a pulse emission, while with sustained emissions, the atmosphere is constantly replenished with these short-lived climate forcers.

3.4.2. Regional emission metrics

A clear coherency between the geographical pattern in the radiative forcing and in the temperature response does not exist. The reason is that transport in the atmosphere and ocean will relocate the energy, and the regional/local responses are to a large degree affected by regional/local feedback mechanisms (Boer and Yu, 2003). Recent research (Shindell and Faluvegi, 2009; Shindell, 2012) have utilized climate models to study and quantify the relationship between radiative forcing in a latitude band (at least 30° wide) and the temperature response in this and other latitude bands. Shindell has developed a concept with coefficients for regional temperature responses (Shindell, 2012), and this method has been applied in this project to indicate the latitudinal distribution in the temperature response, the so-called Regional Temperature change Potentials (RTP), in the same manner as in Collins et al. (2013). The coefficients for BC and ozone are based on Shindell and Faluvegi (2010) and are shown in Table 3 in Collins et al. (2013), while coefficients for SO_4, OC, and methane are based on the average of the coefficients of CO_2 and SO_4 (Shindell and Faluvegi, 2010). RTP is the normalized version of ARTP relative to the reference gas CO_2. While GTP is a global emission metric based on global temperature, RTP is a regional emission metric based on temperatures in different regions. An important aspect is that these calculations are based on new and so far not very extensive research. Different climate models will most likely give significantly different numbers for the regional emission metrics. Hence, the results presented later in this report, with the coefficients from Shindell (2012), should be applied with care.

4. Results

Global averages of atmospheric column and radiative forcing resulting from emissions of particles and ozone precursors for the four Norwegian regions are given in Table 2. Emission metrics for each component are presented in the sub sections.

Table 2. Global and annual means (average of 2006 and 2007) of atmospheric column (µg m^{-2}, for ozone: mDU[4]) and radiative forcing (mW m^{-2}) resulting from emissions in four Norwegian regions. A comparison with the results in the project ArcAct[5] is possible by going to Table 2 in Ødemark et al. (2012).

	Atmospheric column (µg m^{-2}, for O_3: mDU)				Radiative forcing (mW m^{-2})			
Component	East	North	Offshore	West	East	North	Offshore	West
Sulphate	0.049	0.053	0.031	0.034	-0.010	-0.010	-0.006	-0.007
BC air	0.064	0.045	0.032	0.038	0.091	0.061	0.043	0.053
BC snow/ice					0.069	0.070	0.063	0.062
OC	0.153	0.065	0.012	0.063	-0.016	-0.006	-0.001	-0.007
Ozone: CO	0.220	0.077	0.021	0.094	0.008	0.003	0.001	0.004
Ozone: NOx	0.562	0.476	1.430	0.374	0.013	0.011	0.037	0.009
Ozone: nmVOC	0.494	0.158	0.093	0.360	0.012	0.004	0.002	0.009
Methane indir.: CO					0.026	0.009	0.002	0.011
Methane indir.: NOx					-0.035	-0.032	-0.100	-0.025
Methane indir.: nmVOC					0.007	0.002	0.002	0.006

Among the ozone precursors, we see from Table 2 that the NO_X emissions lead to the strongest radiative forcing from ozone for all four regions, with a maximum of 0.037 mW m^{-2} for the Offshore region. However, the net effect of NO_X emissions is a negative radiative forcing for all regions, as NO_X increases OH and, thus, reduces the lifetime of methane. Emissions of CO and nmVOC give a positive radiative forcing both through an increase in ozone and a decrease in OH which leads to a longer methane lifetime. For the aerosols, BC leads to a relative large positive radiative forcing, both through the direct effect and the deposition on snow and ice. The ratio between these two effects varies, with East giving the largest radiative forcing from BC in the atmosphere relative to BC deposited in snow/ice. For the other regions, the results show that the albedo effect is more important than the direct atmospheric effect. OC and sulphate give a weaker radiative forcing, but with an opposite sign of BC.

[4] Milli (10^{-3}) Dobson Units

[5] NFR project: «Unlocking the Arctic Ocean: The climate impact of increased shipping and petroleum activities (ArcAct)»

4.1. Ozone precursors

This section presents the emission metrics for the ozone precursors NO_x, CO, and nmVOC. Global emission metrics for CH_4 are given later in the report.

4.1.1. Global emission metrics

GWP and GTP values for different regions, components and seasons for pulse emissions are presented in Table 3 for time horizons of 20, 100, and 500 years for GWP, and 5, 10, 20, and 50 years for GTP. CO_2 equivalent emissions are given for the same time horizons in Table 4. Results for all time horizons between 0 and 500 years, in addition to GWP and GTP values for the ramp up emissions followed by constant emissions, are available in Annex 1 (the Excel sheet «GWP_GTP_pulse_scenario_ENGLISH.xlsx»). When doing a comparison of emission metrics with other studies, one must take into consideration that the unit of emissions might differ and, thus, must be corrected for. This issue is especially relevant for NO_x, VOC, and SO_2. The emission metrics are adjusted by comparing the atomic weight of the different emission units. For instance, emissions of NO_x are often given for mass of N (Fuglestvedt et al., 2010; Aamaas et al., 2012; Fry et al., 2012; Aamaas et al., 2013; Collins et al., 2013), while here mass of NO_2 is utilized. The conversion from the emission metric for NO_2 (VF_{NO2}) to the emission metric for N (VF_N) is applied by multiplying the atomic weight of nitrogen (V_N = 14 **u**) and dividing on the molecular weight of NO_2 (V_{NO2} = 46 **u**):

$$VF_N = VF_{NO_2} \times \frac{V_{NO_2}}{V_N}$$

Emissions of nmVOC in this report are given per mass of nmVOC, while Aamaas et al. (2012) presented values per mass of C. To convert from per mass of C to per mass of nmVOC, the emission metric must be multiplied by a factor of 0.6.

Table 3. GWP and GTP values (no unit) for different time horizons (for pulse emissions). Emission units (i.e. the molecular weight) utilized in the calculations are CO, NO_2 and nmVOC for emissions of CO, NO_X, and nmVOC, respectively. The emission metrics are presented for the time horizons that historically have been used by IPCC and others. Emission metrics for other time horizons are available in the Excel sheet GWP_GTP_pulse_scenario_ENGLISH.xlsx. As a comparison, we show (in the bottom of the table) global values based on parameters presented in Fuglestvedt et al. (2010). For NO_x, the emission metrics are given for the emission unit NO_2, hence, the global values are lower than those presented in Aamaas et al. (2012) by a factor of 14/46. For nmVOC, the emission metrics are given for the emission unit per mass of nmVOC and not per mass C, thus, the global values are here 40% lower than those presented in Aamaas et al. (2012).

			GWP			GTP			
Region	Component	Season	20 yrs	100 yrs	500 yrs	5 yrs	10 yrs	20 yrs	50 yrs
East	CO	Winter	4.4	1.4	0.4	7.4	5.3	3.0	0.6
		Spring	10.8	3.5	1.1	18.8	12.9	7.2	1.3
		Summer	11.3	3.6	1.1	21.2	13.4	7.1	1.3
		Autumn	4.2	1.4	0.4	7.3	5.0	2.8	0.5
		Annual	**7.2**	**2.3**	**0.7**	**12.8**	**8.6**	**4.8**	**0.9**
	NO_X	Winter	-10.4	-3.3	-1.0	-19.4	-12.3	-6.5	-1.2
		Spring	-21.5	-8.3	-2.5	-6.8	-29.2	-25.5	-4.9
		Summer	-38.3	-15.0	-4.6	-6.8	-52.5	-47.2	-9.2
		Autumn	-12.8	-4.8	-1.5	-6.1	-17.1	-14.4	-2.8
		Annual	**-18.2**	**-7.0**	**-2.1**	**-6.3**	**-24.5**	**-21.3**	**-4.1**
	nmVOC	Winter	10.4	3.1	0.9	25.9	11.5	4.2	0.7
		Spring	15.3	4.5	1.4	38.4	17.0	6.1	1.0
		Summer	15.3	4.8	1.5	30.6	17.9	8.9	1.6
		Autumn	9.9	3.1	0.9	20.5	11.4	5.4	1.0
		Annual	**12.5**	**3.8**	**1.2**	**28.6**	**14.2**	**5.9**	**1.0**
North	CO	Winter	4.6	1.5	0.5	7.8	5.6	3.2	0.6
		Spring	10.4	3.4	1.0	18.1	12.4	6.9	1.3
		Summer	11.5	3.7	1.1	21.4	13.6	7.3	1.3
		Autumn	4.1	1.3	0.4	7.1	4.8	2.7	0.5
		Annual	**7.2**	**2.4**	**0.7**	**12.8**	**8.6**	**4.8**	**0.9**
	NO_X	Winter	-12.2	-4.0	-1.2	-21.3	-14.6	-8.2	-1.5
		Spring	-38.2	-14.6	-4.4	-13.7	-51.5	-44.5	-8.6
		Summer	-58.6	-22.5	-6.8	-20.3	-79.2	-68.7	-13.3
		Autumn	-19.4	-7.2	-2.2	-12.2	-25.6	-20.7	-4.0
		Annual	**-28.3**	**-10.8**	**-3.3**	**-11.5**	**-38.0**	**-32.5**	**-6.3**
	nmVOC	Winter	9.1	2.6	0.8	24.6	9.9	3.0	0.5
		Spring	15.1	4.5	1.4	37.3	16.8	6.2	1.0
		Summer	14.4	4.6	1.4	27.0	16.9	8.9	1.6
		Autumn	9.2	2.9	0.9	18.7	10.6	5.2	0.9
		Annual	**11.7**	**3.5**	**1.1**	**26.6**	**13.2**	**5.5**	**1.0**

The table continues on next page.

Table 3. (Continued from previous page.)

			GWP			GTP			
Region	Component	Season	20 yrs	100 yrs	500 yrs	5 yrs	10 yrs	20 yrs	50 yrs
Offshore	CO	Winter	5.7	1.9	0.6	9.5	6.9	4.0	0,7
		Spring	10.0	3.2	1.0	17.9	11.9	6.5	1,2
		Summer	8.2	2.6	0.8	15.6	9.7	5.0	0,9
		Autumn	5.0	1.6	0.5	8.9	6.0	3.3	0,6
		Annual	**7.3**	**2.3**	**0.7**	**13.0**	**8.6**	**4.8**	**0,9**
	NO_X	Winter	-10.4	-3.5	-1.1	-14.3	-12.8	-8.3	-1,6
		Spring	-26.3	-10.3	-3.1	-3.6	-36.2	-32.8	-6,4
		Summer	-40.2	-15.3	-4.6	-16.7	-53.9	-46.0	-8,9
		Autumn	-15.8	-6.0	-1.8	-7.1	-21.2	-17.9	-3,5
		Annual	**-20.9**	**-8.0**	**-2.4**	**-7.1**	**-28.2**	**-24.5**	**-4,7**
	nmVOC	Winter	9.9	3.0	0.9	22.3	11.2	4.8	0,8
		Spring	15.2	4.6	1.4	35.9	17.1	6.8	1,2
		Summer	12.3	3.9	1.2	24.3	14.3	7.2	1,3
		Autumn	9.0	2.8	0.9	17.7	10.5	5.3	0,9
		Annual	**11.5**	**3.5**	**1.1**	**24.9**	**13.2**	**5.9**	**1,0**
West	CO	Winter	4.5	1.5	0.4	7.6	5.4	3.1	0,6
		Spring	10.6	3.4	1.0	18.5	12.6	7.0	1,3
		Summer	10.9	3.5	1.1	20.5	12.8	6.8	1,2
		Autumn	4.4	1.4	0.4	7.8	5.2	2.9	0,5
		Annual	**7.3**	**2.3**	**0.7**	**12.9**	**8.6**	**4.8**	**0,9**
	NO_X	Winter	-13.6	-4.6	-1.4	-18.6	-16.8	-10.9	-2,0
		Spring	-21.6	-8.4	-2.6	-3.7	-29.6	-26.7	-5,2
		Summer	-35.4	-13.7	-4.2	-9.8	-48.1	-42.3	-8,2
		Autumn	-14.4	-5.6	-1.7	-3.9	-19.6	-17.2	-3,3
		Annual	**-19.2**	**-7.4**	**-2.2**	**-6.2**	**-26.0**	**-22.6**	**-4,4**
	nmVOC	Winter	11.1	3.3	1.0	26.7	12.4	4.7	0,8
		Spring	15.2	4.5	1.4	37.7	16.9	6.1	1,0
		Summer	14.5	4.5	1.4	29.7	16.7	8.0	1,4
		Autumn	10.1	3.1	1.0	20.9	11.7	5.5	1,0
		Annual	**12.6**	**3.8**	**1.2**	**28.6**	**14.2**	**6.0**	**1,0**
Norway	CO	**Annual**	7.2	2.3	0.7	12.8	8.6	4.8	0,9
Norway	NO_X	**Annual**	-20.5	-7.8	-2.4	-7.1	-27.6	-24.0	-4,6
Norway	nmVOC	**Annual**	12.3	3.7	1.1	28.0	14.0	5.9	1,0
Emission metrics for global emissions									
NOx, surface			-26.2	-11.1	-3.4	16.5	-38.3	-39.9	-7.8
NOx, aircraft (Wild et al., 2001)			122	21.1	6.4	612	105	-62.9	-18.5
NOx, shipping			-98.2	-37.4	-11.4	-40.9	-131.9	-112.6	-21.8
CO, surface (Derwent et al., 2001)			6.0	2.0	0.6	11.4	6.9	3.7	0.8
nmVOC, surface (Collins et al., 2002)			8.6	2.7	0.8	18.8	9.8	4.5	0.9

Table 4. Emissions given in CO_2 equivalents (kt) for GWP and GTP and for different time horizons (for pulse emissions). Emissions in CO_2 equivalents are calculated by multiplying the emission metric (*M*) with emissions (*E*), $CO_2\text{-}ek(t)=M_x(t)*E_x$. The emission units utilized in the calculations are kt(CO), kt(NO_2), and kt(nmVOC) for emissions of CO, NO_X, and nmVOC, respectively. The total Norwegian emissions (Table 1) in CO_2 equivalents are estimated as the sum of the different regions and seasons, which can give a different number than multiplying Norwegian emissions with the emission metric for Norway.

			GWP, CO_2 equivalents (kt)			GTP, CO_2 equivalents (kt)			
Region	Component	Season	20 yrs	100 yrs	500 yrs	5 yrs	10 yrs	20 yrs	50 yrs
East	CO	Winter	239	78	24	404	286	164	30
		Spring	490	160	48	856	585	328	60
		Summer	333	106	32	622	392	207	38
		Autumn	163	53	16	287	195	108	20
	NO_X	Winter	-97	-31	-9	-182	-115	-61	-11
		Spring	-201	-78	-24	-64	-273	-238	-46
		Summer	-347	-135	-41	-62	-475	-427	-83
		Autumn	-117	-44	-13	-56	-156	-131	-25
	nmVOC	Winter	165	48	15	410	182	66	11
		Spring	238	70	21	596	264	95	16
		Summer	221	70	21	441	258	128	23
		Autumn	147	46	14	306	170	81	14
North	CO	Winter	87	29	9	147	104	60	11
		Spring	176	57	17	307	210	117	21
		Summer	123	40	12	228	146	78	14
		Autumn	59	19	6	103	70	39	7
	NO_X	Winter	-68	-22	-7	-119	-82	-46	-8
		Spring	-217	-83	-25	-78	-292	-253	-49
		Summer	-327	-126	-38	-113	-442	-383	-74
		Autumn	-108	-40	-12	-68	-143	-116	-22
	nmVOC	Winter	48	14	4	130	53	16	3
		Spring	80	24	7	196	89	33	5
		Summer	69	22	7	131	82	43	8
		Autumn	46	14	4	95	54	26	5
Offshore	CO	Winter	21	7	2	35	25	15	3
		Spring	38	12	4	67	45	25	4
		Summer	31	10	3	58	36	19	3
		Autumn	19	6	2	33	22	12	2
	NO_X	Winter	-233	-79	-24	-320	-288	-187	-35
		Spring	-604	-237	-72	-83	-830	-752	-146
		Summer	-920	-350	-107	-382	-1236	-1055	-204
		Autumn	-358	-136	-41	-162	-479	-406	-78
	nmVOC	Winter	28	9	3	64	32	14	2
		Spring	44	13	4	105	50	20	3
		Summer	36	11	3	71	42	21	4
		Autumn	26	8	2	51	30	15	3

The table continues on next page.

Table 4. (Continued from previous page.)

Region	Component	Season	GWP, CO_2 equivalents (kt) 20 yrs	100 yrs	500 yrs	GTP, CO_2 equivalents (kt) 5 yrs	10 yrs	20 yrs	50 yrs
West	CO	Winter	98	32	10	167	117	67	12
		Spring	202	66	20	353	241	135	25
		Summer	141	45	14	265	166	87	16
		Autumn	70	23	7	123	83	46	8
	NO_X	Winter	-82	-28	-9	-113	-102	-66	-12
		Spring	-133	-52	-16	-23	-182	-164	-32
		Summer	-213	-82	-25	-59	-289	-254	-49
		Autumn	-87	-33	-10	-24	-118	-104	-20
	nmVOC	Winter	126	38	11	305	141	54	9
		Spring	173	51	16	431	193	70	12
		Summer	159	49	15	326	184	88	16
		Autumn	112	35	11	232	129	61	11
Norway	CO	Annual	2288	742	226	4056	2723	1508	276
	NO_X	Annual	-4112	-1557	474	-1905	-5500	-4643	-896
	nmVOC	Annual	1719	522	159	3889	1951	831	144

Emissions of CO and nmVOC both lead to positive GWP and GTP values (warming) for all regions, time horizons and seasons (see Table 3). The importance of season is rather similar for these two components, with higher GWP values in the spring and summer than in the autumn and winter. This result is illustrated for CO in Figure 2 and is caused mainly because ozone production efficiency increase with sunlight - The emissions metrics decrease rapidly with increasing time horizon.

The effects of NO_x emissions are more complex and give negative GWP values (cooling) for emissions during all seasons for time horizons longer than approximately 5 years (Figure 2). NO_x emissions lead, in general, to more OH, which reduce the lifetime of the greenhouse gas methane. Hence, this chemical reaction has a cooling effect which in this case dominates over the warming effect from increased ozone concentrations. For very short time horizons (shorter than about 5 years), the NO_x emissions lead to positive GWP values for all seasons, except in winter. This exception occurs since NO_x emissions in winter leads to less ozone due to little access to sunlight (titration effect, $NO+O_3 \rightarrow NO_2+O_2$). The photochemistry is faster in summer than in winter; hence, the ozone production is larger in summer.

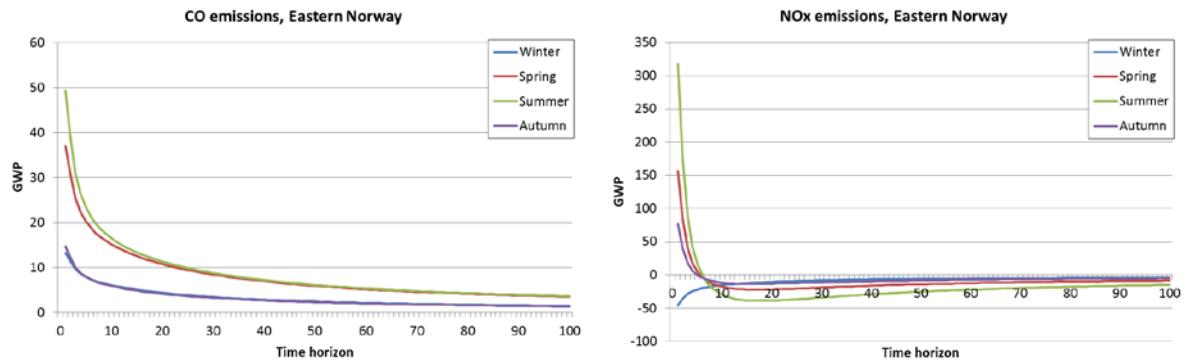

Figure 2. GWP values as a function of time horizon for CO (left) and NO_X (right) in Eastern Norway for each season.

4.1.2. Regional emission metrics

Regional temperature responses calculated for each of the ozone precursors are presented in Figure 3 for 20 and 100 years' time horizons. Unfortunately, we do not have data accessible to estimate these responses for a time horizon of 10 years. These regional temperature responses are based on the emission metric Absolute Regional Temperature Response (ARTP). The methodology is the same as in Collins et al. (2013) (see Section 3.4.2) except for that the effect of ozone precursors on sulphate is not taken into account, however, this effect is relatively small (see Figure 4 in Collins et al. (2013)) in relation to the effect of ozone precursors on ozone and methane (Shindell et al., 2009). Contrary to the calculated global emission metrics (Section 4.1.1), the effect of changes in stratospheric water vapour is not included here, as information on the latitudinal distribution of this effect is lacking (Collins et al., 2013). We do not know how large this effect is regionally. The latitudinal distribution of the radiative forcing of methane is not accessible in our calculations; however, this distribution is taken from Collins et al. (2013). That study is based on model runs with and without a reduction of 20% in the mixing ratio of methane (see Fry et al. (2012)) and has the following distribution: -85, -141, -107, and -76 mW m^{-2} for the latitudinal bands 90°S-28°S, 28°S-28°N, 28°N-60°N, and 60°N-90°N, respectively.

We see from Figure 3 that the response in each latitudinal band is relative similar for emissions in the four different regions. This similarity occurs since radiative forcing in the latitudinal bands are similar as the four emission regions in Norway are quite close to each other in comparison to the resolution in the method by Shindell et al. NO_x in Northern Norway stands out, with generally higher negative values than for emissions from other regions, a signal that was seen for the global emission metrics as well (Section 4.1.1). For all four regions, the response in ARTP(20) is strongest in the latitudinal band 28°N-60°N for emissions of CO and nmVOC, while strongest in the Tropics (28°S-28°N) for emissions of NO_X. Since the methane response operates on a global scale, one can expect results like this, i.e. a response in the Tropics. As described in Collins et al. (2013), the long-term effect (methane and methane induced ozone) dominates for ARTP(20), while short-term ozone actually contributes to create a balance with the long-term effects for ARTP(100). The long-term effects will no matter what dominate far from the location of the emissions, thus, ARTP(100) for Norwegian emissions will have most negative values in the latitudinal band 90°S-28°S. In summary, Figure 3 shows that there are variations in the response pattern behind the global average value, and the Shindell method used here give indications of how this pattern may be. In addition, the figure shows how much the regional response deviates from the global average value.

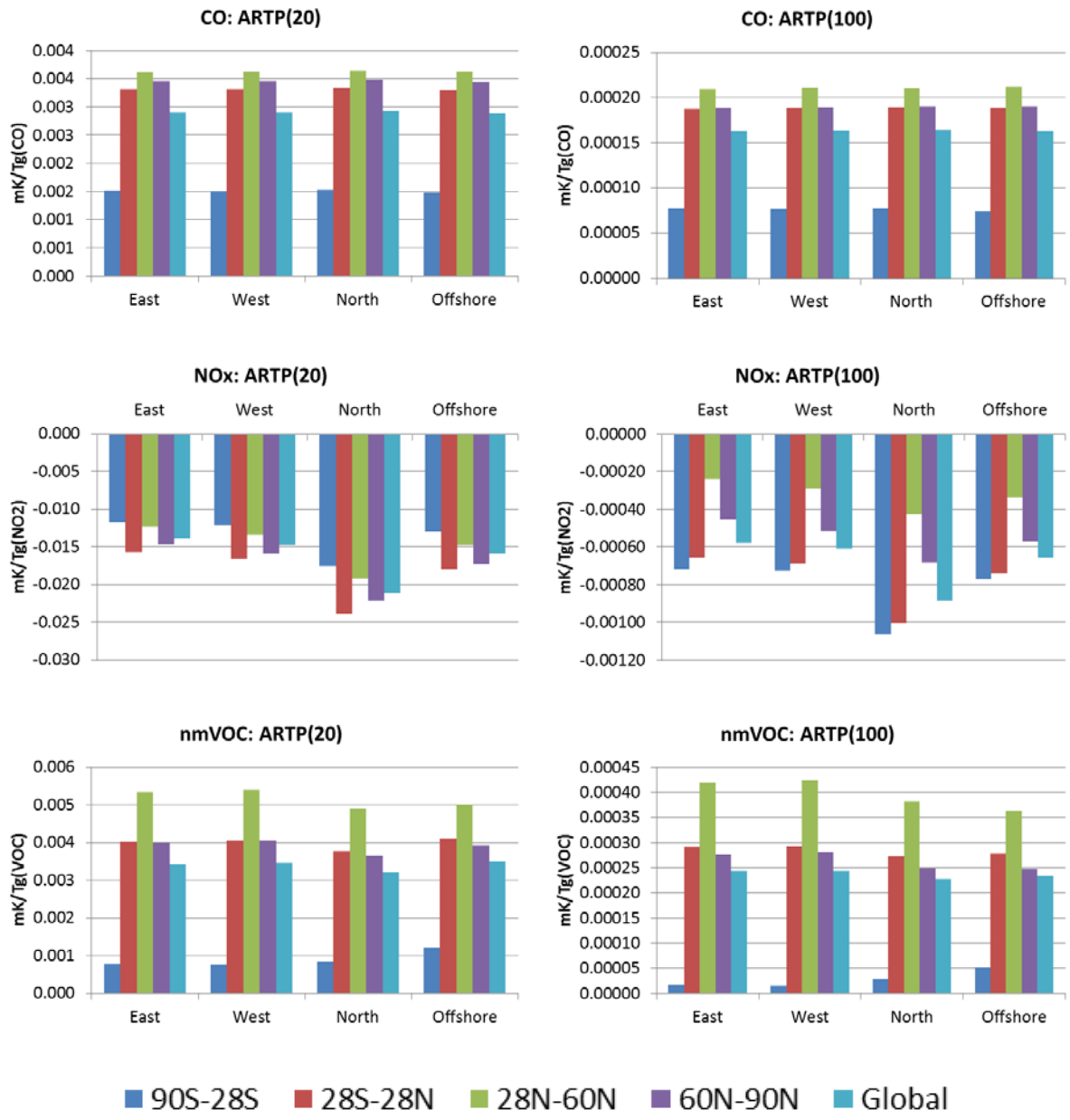

Figure 3. ARTP values for time horizons of 20 years (left) and 100 years (right) for pulse emissions of ozone precursors in the four Norwegian regions. The unit is milli Kelvin per million ton of the component, mK/Tg(CO), mK/Tg(NO_2) and mK/Tg(nmVOC) for emissions of CO, NO_X and nmVOC, respectively. The columns show the temperature response in 4 different latitudinal bands (90°S-28°S, 28°S-28°N, 28°N-60°N, 60°N-90°N) and globally. Please notice that the scale varies between the six diagrams.

4.1.3. Concentrations near the surface

Ozone is a poisonous gas for humans, animals, and plants, thus, studying the impact of Norwegian emissions of ozone precursors on the ozone concentration near the surface in addition to the climate impact in the troposphere is therefore appropriate. The figures presented in this section are based on calculations with the Oslo CTM2 model (the same as described above), i.e. for the meteorological

years in 2006 and 2007 and with emissions for 2010. In the model runs, ozone concentrations in the lowest layer in the model, which represents approximately 8 m over surface level, are saved every third hour. Based on these data, a maximum value for every day was calculated, and these daily maximum values have been averaged over time over the summer season (June, July, and August). The two top figures show total produced ozone in Norway and ozone formed due to emissions outside of Norway or from natural sources. For the figures that show the difference in ozone concentrations, the values represents a 100% perturbation (the difference between the reference and Norwegian emissions removed) of emissions for one or more ozone precursors/regions. Even though the horizontal resolution (T42) is relatively crude when it comes to studies of local air pollution, the Oslo CTM2 model has shown in previous studies a decent match for this resolution with measurements of ozone and NO_2 in Europe (Colette et al., 2011). We present here the ozone mixing ratios in ppb. This can be converted into concentration ($\mu g/m^3$) by multiplying with a factor 2.

Figure 4 (top) shows that the daily maximum of ozone concentrations near the surface in Norway is between 30 and 45 parts per billion (ppb) for the summers both in 2006 and 2007, and that the values are generally highest in the south and lowest in the north. The effect on ozone for emissions of all ozone precursors emitted in Norway (Figure 4, bottom) seems to be largest along and outside of the coast in Western Norway and Central Norway with maximum values of about 1.5 ppb. Norwegian emissions contribute with maximum 3-4% of the seasonal average of daily maximum values of ozone. The differences between 2006 and 2007 are small here also, and we will therefore give the average of the two years in the following figures (Figures 5 and 6).

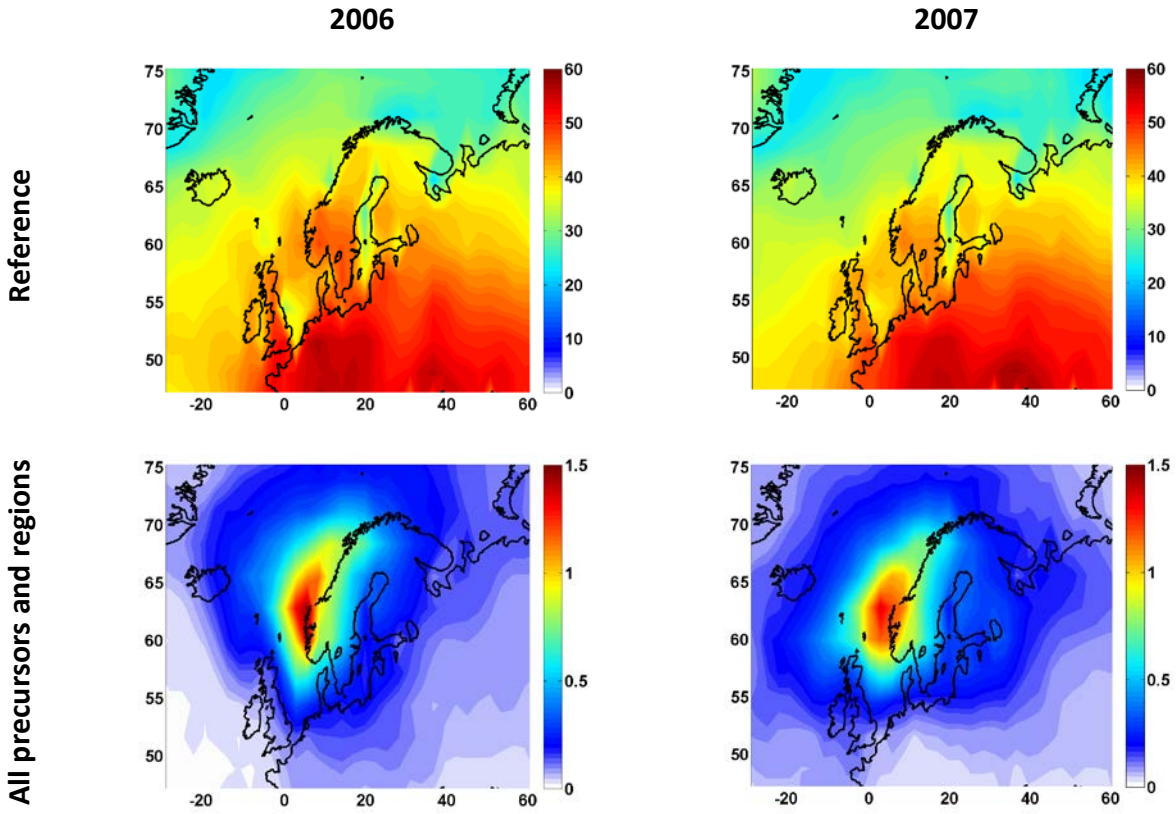

Figure 4. Daily maximum values for ozone mixing ratios (ppb) near the surface in the summer (average of June, July, and August) modelled with Oslo CTM2 with meteorology from 2006 (left column) and 2007 (right column). The two upper figures show the results from the reference simulation, where all global emissions are included (see Section 3.2), while the two lower figures show the effect of Norwegian emissions on ozone (i.e. emissions of CO, NO_X and nmVOC from all four Norwegian regions).

Figure 5 shows the effect of NO_X emissions on ozone, given separately for emissions from each of the four regions. These figures have been generated by finding the difference between the reference simulation and simulations where emissions from one region at the time is removed. We observe here that emissions of NO_X from the offshore region contribute at the most with a little less than 1 ppb ozone and this region/component is responsible for most of the changes of local ozone due to emissions in Norway (Figure 4, bottom). Emissions of NO_X in the three other regions are lower and give therefore a smaller increase in ozone relative to the offshore region (Figure 5). The lifetime of ozone is also shorter over land due to uptake from vegetation. Due to the short lifetime of NO_X (from a few hours in the boundary layer to a few days in upper troposphere (e.g., Zhang et al., 2003)), the changes in ozone are largest in the vicinity of the location of the emissions in each of the four regions.

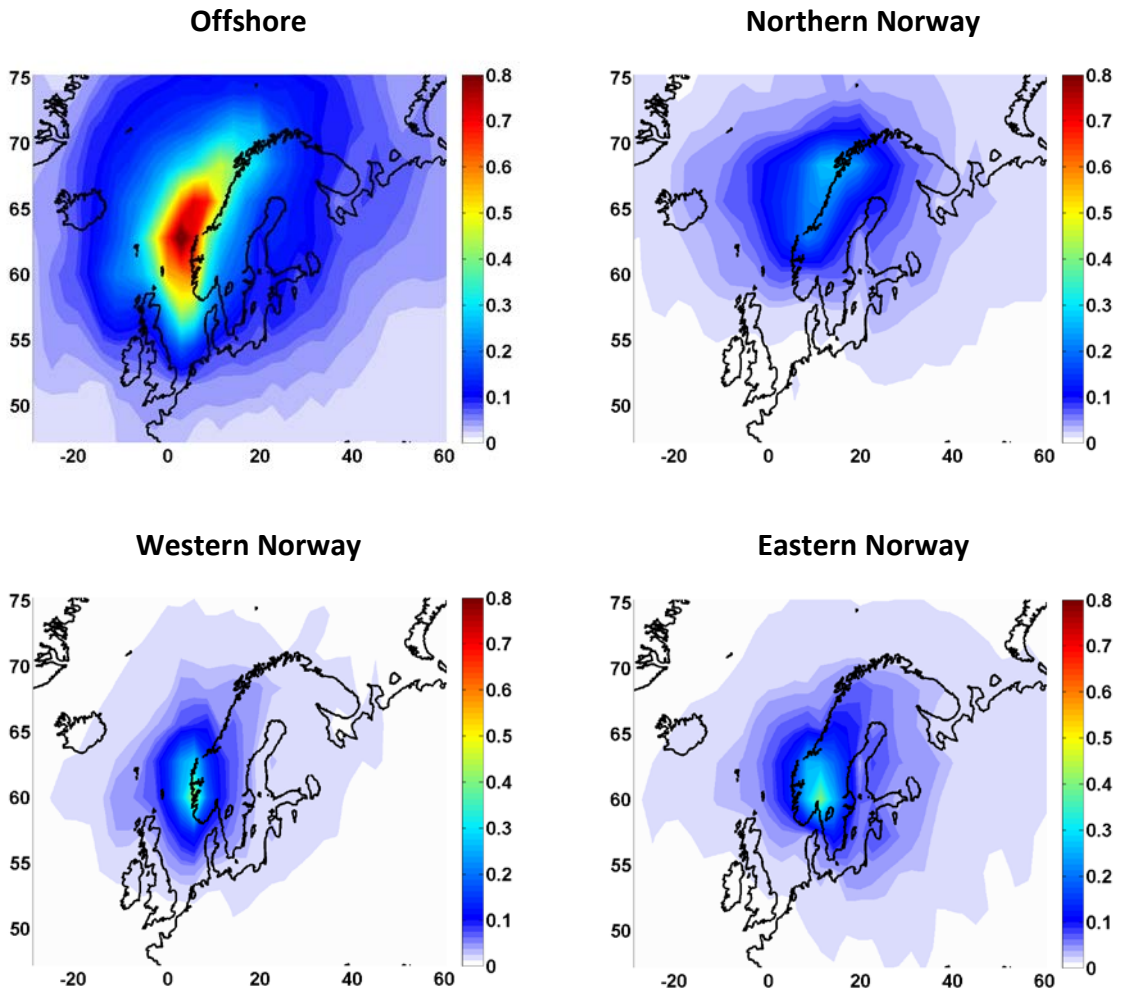

Figure 5. The difference in daily maximum values of ozone concentrations (ppb) due to emissions of NO_x in each of the four regions in Norway. For ozone concentrations in µg/m^3, multiply with 2. The figures show the difference in concentrations near the surface in the summer, modelled with Oslo CTM2, and is an average of the simulations run with meteorology from 2006 and 2007.

CO and many nmVOCs have longer lifetimes than NO_x, thus, emissions of these precursors in Norway will lead to an increase in ground level ozone over a larger area. But, emissions of NO_x will locally result in a much larger increase of ozone concentrations than for other ozone precursors. Figure 6 shows the effect on ozone of emissions from Eastern Norway, and we model that the maximal effect here is about 7 and 60 parts per trillion (ppt) for emissions of CO and nmVOC, respectively. Since the lifetimes are somewhat longer over ocean than over land, the ozone concentrations will be largest south of the emission locations, thus, over Skagerrak and the North Sea. Due to non-linear chemistry, it is difficult to assess which ozone precursors contribute the most to ozone formation and to what degree, but emissions of NO_x have a larger impact than emissions of CO and nmVOC both nationally and globally (Jacob, 1999).

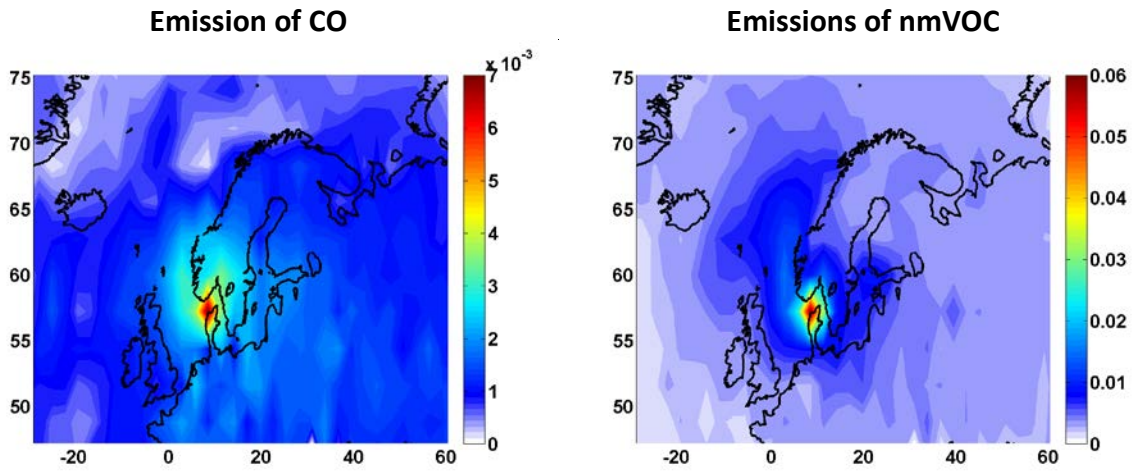

Figure 6. Difference in daily maximum values of ozone concentrations (ppb) due to emissions of CO (left) and nmVOC (right) in Eastern Norway. For ozone concentrations in µg/m^3, multiply with 2. The figures show the difference in concentrations near the surface in the summer, modelled with Oslo CTM2, and is an average of the simulations run with meteorology from 2006 and 2007. Please notice that the scale is different in the two figures.

4.1.4. Uncertainties in calculations of emission metrics

Data from the literature are utilized to estimate the uncertainty in the chemistry modelling that is used as input in the emission metrics calculations. The uncertainty in the emission metrics here are based only on the uncertainty in the chemical processes, not uncertainty in relation to CO_2 or the temperature response. For a time horizon of 20 years (time horizon of 100 years in parenthesis), the GWP values in Tables 3 and 4 will have a roughly uncertainty (for 1 sigma) of ±28%, (±27%), 45% (±45%) and ±41% (±47%) for CO, NO_X, and nmVOC, respectively (Fry et al., 2012). The uncertainties in the GTP values for a time horizon of 20 years are estimated to ±38%, ±31% and 68% for CO, NO_X, and nmVOC, respectively (Collins et al., 2013). Collins et al. (2013) have not provided uncertainties for a time horizon of 10 years. Figure 7 illustrates the uncertainty in GTP(20) for emissions of each of the three ozone precursors in Eastern Norway in the summer. The figure does therefore not show the total uncertainty for GTP (see below), for instance, uncertainty in the reference gas CO_2 is not included, but this figure illustrates the importance of uncertainties in the chemical modelling for GTP(20).

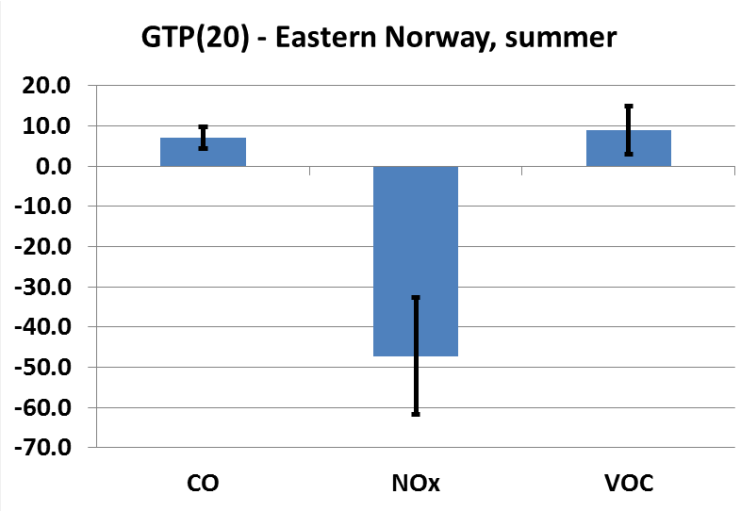

Figure 7. GTP values for time horizon of 20 years for emissions from Eastern Norway during the summer season. The vertical lines present estimated uncertainty for the different components.

In this project, we have performed CTM modelling for two meteorological years, 2006 and 2007, in order to reduce uncertainty. A comparison of the radiative forcing per kg of emission shows that the difference in results between those two years are relatively small on an annual basis – in the order of 5-15% for most of the ozone precursors/regions even though these years were very different when it comes to the meteorological conditions, while the differences increases substantially when comparing results for seasons.

In addition to the uncertainty in the chemical modelling mentioned above, uncertainty appear also related to emissions, as well as calculations of radiative forcing and emission metrics (e.g., $AGWP_{CO2}$ (Joos et al., 2013)). Further, changes in concentrations of certain gases may cause changes in the carbon cycle, which will impact the climate (e.g., Sitch et al., 2007). Collins et al. (2010) studied the effect of ground level ozone on vegetation and found that the reduced uptake of CO_2 (as a result of increased ozone concentrations and therefore damages on vegetation) lead to a 10% increase in GTP(20) for methane. This effect can contribute to a change of sign for many different time horizons of GTP for emissions of NO_x and, thus, increase the uncertainty linked to this gas. Another effect that will contribute to cooling is that emissions of NO_x may generate nitrate particles in areas with large amounts of NH_3 (Bauer et al., 2007). The effect of ozone precursors on OH, and, hence, the oxidation of sulphurdioxide (SO_2), can also lead to changes in sulphate particles. This effect seems to be relatively small in comparison to the effect of ozone precursors on ozone and methane, but the uncertainty in the CTM calculations are large when it comes to the size and sign of the sulphate effect from the ozone precursors (Fry et al., 2012).

In the GTP and RTP calculations, an additional large uncertainty is connected to the temperature response function, and especially to the latitudinal distribution which is applied in the calculations of RTP. The uncertainty increases as one goes from GWP to GTP as the emission metric must then also include a function that describes the temperature response due to a radiative forcing.

4.2. Aerosols

In this section, we present emission metrics for aerosols due to emissions of BC, OC, and SO_2.

4.2.1. Global emission metrics

GWP and GTP values for different regions and seasons are presented for emissions of BC, OC, and SO_2 in Table 5 for time horizons of 20, 100, and 500 years for GWP, and 5, 10, 20, and 50 years for GTP. CO_2-equivalent emissions are given in Table 6 for the same time horizons. The emissions metrics are shown with time horizons that historically have been used by the IPCC and others. The results for all time horizons between 0 and 500 years are available in Annex 1 («GWP_GTP_pulse_scenario_ENGLISH.xlsx»). Emissions of SO_2 are in this report given per mass SO_2, not per mass S. One must multiply the emission metric with a factor 2 to go from SO_2 to S. The emission metrics have been compared to those values for petroleum activity in the Arctic (Ødemark et al., 2012). Since the models and model setup are relatively similar to Ødemark et al. (2012), a comparison between what we found for offshore with the petroleum activities in the Arctic is in place. However, some differences in the results are expected, e.g., since the emissions occur in different latitudes and variations in the emission dataset.

BC is dark particles that absorb incoming solar radiation. We have split the emission metric into two for BC, 1) the direct effect in the atmosphere and 2) the albedo effect on snow and ice. The total climate effect is the sum of the emission metrics for these two effects. (Other effects are linked to BC. These effects are related to formation and properties of clouds and are labelled as indirect effects. See Bond et al. (2013) for a discussion and quantification of these effects.) In the atmosphere, BC particles absorb solar radiation. Deposition of the black BC particles on the ground leads to light surfaces of snow and ice becoming greyer, i.e. reduced albedo as less radiation is reflected. The emission metrics for the direct effect are largest for emissions in Eastern Norway, but the variation between the different regions is small. The differences are much larger between seasons, where the emission metrics are largest in summer and spring when elevation of the sun is high and the days are long. The same seasonal variation is also observed for the albedo effect. Even though the area covered with snow and ice is largest in winter, the emission metric values are largest when the solar radiation is at its strongest. While the albedo effect is approximately 10-15% of the direct effect for global emissions (Rypdal et al., 2009; Bond et al., 2011), Norwegian emissions lead to relatively higher contribution from the albedo effect than for global emissions (77-146%). The cause is that parts of the Norwegian emissions are transported to the Arctic and that snow and ice covers large parts of Norway for many months every winter. The contribution from the albedo effect relative to the contribution from the direct effect over a year is largest for offshore (146%) and smallest for Eastern Norway (77%). The seasonal variations are large, with largest relative contribution for the albedo effect in winter, closely followed by spring and summer, and the smallest relative contribution in autumn. The coverage of snow and ice is smallest in the autumn, which can explain the relatively small impact of the albedo effect in the autumn. In winter, the incoming solar radiation is small and the extent of snow large, which contribute to a relative large share for the albedo effect compared to the direct effect. Emissions in the Arctic (with a definition similar to what AMAP uses, and where very little of mainland Norway is included) will have a much stronger relative albedo

effect (Ødemark et al., 2012), since the locations of Norwegian emissions are much further away from snow and ice covered areas in the Arctic.

OC are light particles which scatter incoming solar radiation, and, thus, lead to a cooling. For OC, the emission metric values are largest for emissions from offshore, while smallest in Northern Norway. The seasonal variations are much larger than the variations between the regions, as for BC. The cooling effect is largest in summer, when the incoming solar radiation is largest and the number of sun hours is largest. The values for OC can be converted to values for organic matter (OM) by multiplying with 1.6. The emissions metrics are similar or a bit lower than for emissions in the Arctic (Ødemark et al., 2012).

Emissions of SO_2 result in formation of sulphate particles in the atmosphere. These particles also scatter incoming solar radiation. The emission metric values are largest for Eastern Norway. The variations are much larger over seasons than between regions. As for OC, the emission metrics are largest in summer, while they are only slightly negative in winter. The emission metric values for aerosols are somewhat lower than for Arctic conditions in Ødemark et al. (2012) since the global chemistry transport model (Oslo CTM2) we have applied is updated with more wet deposition, i.e. precipitation removes particles from the atmosphere, compared to the previous study.

The magnitude of the indirect effect of aerosols is very uncertain. Often, the entire indirect effect is ascribed to SO_2. In AR4, the indirect effect is given as a factor 1.75 of the direct effect of SO_2. Due to large uncertainty, AR4 state that this factor can vary between 0.75 and 4.5 for global emissions.

Table 5. GWP and GTP values for various time horizons for national emissions (for pulse emissions). The unit of emissions (i.e. the «molecule weight») used in the calculations is BC, OC, and SO_2 for emissions of the particles. For BC, the emission metric is divided in the direct effect and the albedo effect. The total emission metric value is the sum of these two effects. In addition, we show (in the bottom of the table) global values based on parameters presented in Fuglestvedt et al. (2010) as a comparison. These global emission metrics are the same as those presented in Aamaas et al. (2012). The albedo effect of BC is here given as 20% of the direct effect (Bond et al., 2013). SO_2 is given per mass SO_2 and not per mass S.

			GWP			GTP			
Region	Component	Season	20 yrs	100 yrs	500 yrs	5 yrs	10 yrs	20 yrs	50 yrs
East	BC (direct effect)	Winter	746	212	64	1867	739	216	36
		Spring	2166	615	187	5423	2148	627	104
		Summer	2414	686	209	6044	2394	699	116
		Autumn	870	247	75	2179	863	252	42
		Annual	**1484**	**422**	**128**	**3716**	**1472**	**430**	**71**
	BC (albedo effect)	Winter	831	236	72	2081	825	241	40
		Spring	1658	471	143	4150	1644	480	80
		Summer	2029	576	175	5079	2012	587	97
		Autumn	205	58	18	512	203	59	10
		Annual	**1137**	**323**	**98**	**2846**	**1127**	**329**	**55**
	OC	Winter	-24	-7	-2	-61	-24	-7	-1
		Spring	-82	-23	-7	-204	-81	-24	-4
		Summer	-182	-52	-16	-455	-180	-53	-9
		Autumn	-50	-14	-4	-126	-50	-15	-2
		Annual	**-64**	**-18**	**-6**	**-160**	**-63**	**-18**	**-3**
	SO_2	Winter	-19	-5	-2	-48	-19	-6	-1
		Spring	-90	-26	-8	-226	-89	-26	-4
		Summer	-187	-53	-16	-468	-185	-54	-9
		Autumn	-55	-16	-5	-137	-54	-16	-3
		Annual	**-86**	**-25**	**-7**	**-216**	**-86**	**-25**	**-4**
North	BC (direct effect)	Winter	684	194	59	1712	678	198	33
		Spring	2017	573	174	5050	2000	584	97
		Summer	2130	605	184	5332	2112	617	102
		Autumn	760	216	66	1904	754	220	37
		Annual	**1381**	**392**	**119**	**3457**	**1370**	**400**	**66**
	BC (albedo effect)	Winter	1249	355	108	3128	1239	362	60
		Spring	2294	652	198	5744	2276	664	110
		Summer	2501	711	216	6263	2481	724	120
		Autumn	367	104	32	918	364	106	18
		Annual	**1587**	**451**	**137**	**3974**	**1574**	**460**	**76**
	OC	Winter	-20	-6	-2	-50	-20	-6	-1
		Spring	-72	-20	-6	-180	-71	-21	-3
		Summer	-137	-39	-12	-343	-136	-40	-7
		Autumn	-37	-11	-3	-93	-37	-11	-2
		Annual	**-55**	**-16**	**-5**	**-138**	**-55**	**-16**	**-3**
	SO_2	Winter	-18	-5	-2	-46	-18	-5	-1
		Spring	-81	-23	-7	-203	-80	-23	-4
		Summer	-148	-42	-13	-370	-146	-43	-7
		Autumn	-39	-11	-3	-97	-38	-11	-2
		Annual	**-72**	**-20**	**-6**	**-180**	**-71**	**-21**	**-3**

The table continues on next page.

Table 5. (Continued from previous page.)

Region	Component	Season	GWP 20 yrs	GWP 100 yrs	GWP 500 yrs	GTP 5 yrs	GTP 10 yrs	GTP 20 yrs	GTP 50 yrs
Offshore	BC (direct effect)	Winter	780	222	67	1953	774	226	37
		Spring	1868	531	161	4676	1852	541	90
		Summer	1794	510	155	4491	1779	519	86
		Autumn	861	245	74	2156	854	249	41
		Annual	**1334**	**379**	**115**	**3341**	**1323**	**386**	**64**
	BC (albedo effect)	Winter	1358	386	117	3400	1347	393	65
		Spring	3094	879	267	7746	3068	896	149
		Summer	2993	850	258	7493	2968	866	144
		Autumn	325	92	28	815	323	94	16
		Annual	**1950**	**554**	**168**	**4882**	**1934**	**565**	**94**
	OC	Winter	-26	-7	-2	-64	-25	-7	-1
		Spring	-75	-21	-6	-187	-74	-22	-4
		Summer	-119	-34	-10	-297	-118	-34	-6
		Autumn	-52	-15	-4	-130	-52	-15	-2
		Annual	**-68**	**-19**	**-6**	**-171**	**-68**	**-20**	**-3**
	SO_2	Winter	-23	-7	-2	-58	-23	-7	-1
		Spring	-75	-21	-7	-189	-75	-22	-4
		Summer	-126	-36	-11	-315	-125	-36	-6
		Autumn	-45	-13	-4	-111	-44	-13	-2
		Annual	**-68**	**-19**	**-6**	**-170**	**-67**	**-20**	**-3**
West	BC (direct effect)	Winter	839	238	72	2100	832	243	40
		Spring	1989	565	172	4980	1973	576	96
		Summer	2065	587	178	5169	2048	598	99
		Autumn	929	264	80	2326	921	269	45
		Annual	**1436**	**408**	**124**	**3595**	**1424**	**416**	**69**
	BC (albedo effect)	Winter	1017	289	88	2546	1009	294	49
		Spring	2609	741	225	6532	2588	755	125
		Summer	2973	845	257	7444	2949	861	143
		Autumn	275	78	24	689	273	80	13
		Annual	**1688**	**480**	**146**	**4227**	**1674**	**489**	**81**
	OC	Winter	-28	-8	-2	-70	-28	-8	-1
		Spring	-77	-22	-7	-193	-77	-22	-4
		Summer	-153	-44	-13	-384	-152	-44	-7
		Autumn	-50	-14	-4	-125	-49	-14	-2
		Annual	**-64**	**-18**	**-6**	**-160**	**-63**	**-18**	**-3**
	SO_2	Winter	-24	-7	-2	-61	-24	-7	-1
		Spring	-80	-23	-7	-201	-80	-23	-4
		Summer	-124	-35	-11	-311	-123	-36	-6
		Autumn	-52	-15	-5	-131	-52	-15	-3
		Annual	**-70**	**-20**	**-6**	**-175**	**-69**	**-20**	**-3**

The table continues on next page.

Table 5. (Continued from previous page.)

			GWP			GTP			
Region	Component	Season	20 yrs	100 yrs	500 yrs	5 yrs	10 yrs	20 yrs	50 yrs
Norway	BC (direct effect)	**Annual**	1420	403	123	3556	1409	411	68
Norway	BC (albedo effect)	**Annual**	1518	431	131	3802	1506	440	73
Norway	OC	**Annual**	-62	-18	-5	-155	-62	-18	-3
Norway	SO_2	**Annual**	-75	-21	-6	-187	-74	-22	-4
Emission metrics for global emissions									
BC (direct effect), global			1595	453	138	3995	1582	462	77
BC (albedo effect), global			319	91	28	799	317	92	15
OC, global			-248	-70	-21	-621	-246	-72	-12
SO_2, global			-143	-41	-12	-358	-142	-41	-6,9

Table 6. Emissions of BC, OC, and SO_2 given as CO_2 equivalents (kt) for GWP and GTP and for various time horizons (for pulse emissions). Emissions in CO_2 equivalents are calculated by multiplying the emission metric (*M*) with emissions (*E*), $CO_2\text{-}ek(t)=M_x(t)*E_x$. The total Norwegian emissions (Table 1) in CO_2 equivalents are calculated as the sum from the different regions and seasons, which can give a slightly different number than if one multiply Norwegian emissions with the emission metric for Norway.

Region	Component	Season	GWP, CO_2 equivalents (kt)			GTP, CO_2 equivalents (kt)			
			20 yrs	100 yrs	500 yrs	5 yrs	10 yrs	20 yrs	50 yrs
East	BC (direct effect)	Winter	559	159	48	1400	555	162	27
		Spring	1430	406	123	3579	1418	414	69
		Summer	1183	336	102	2962	1173	342	57
		Autumn	514	146	44	1286	509	149	25
	BC (albedo effect)	Winter	623	177	54	1561	618	181	30
		Spring	1094	311	95	2739	1085	317	53
		Summer	994	282	86	2489	986	288	48
		Autumn	121	34	10	302	120	35	6
	OC	Winter	-94	-27	-8	-234	-93	-27	-4
		Spring	-231	-66	-20	-578	-229	-67	-11
		Summer	-196	-56	-17	-491	-195	-57	-9
		Autumn	-110	-31	-9	-274	-109	-32	-5
	SO_2	Winter	-24	-7	-2	-61	-24	-7	-1
		Spring	-113	-32	-10	-282	-112	-33	-5
		Summer	-217	-62	-19	-543	-215	-63	-10
		Autumn	-66	-19	-6	-164	-65	-19	-3
North	BC (direct effect)	Winter	335	95	29	839	332	97	16
		Spring	948	269	82	2373	940	274	46
		Summer	852	242	74	2133	845	247	41
		Autumn	335	95	29	838	332	97	16
	BC (albedo effect)	Winter	612	174	53	1533	607	177	29
		Spring	1078	306	93	2700	1070	312	52
		Summer	1001	284	86	2505	992	290	48
		Autumn	161	46	14	404	160	47	8
	OC	Winter	-30	-8	-3	-75	-30	-9	-1
		Spring	-93	-26	-8	-234	-93	-27	-4
		Summer	-84	-24	-7	-209	-83	-24	-4
		Autumn	-38	-11	-3	-95	-38	-11	-2
	SO_2	Winter	-26	-7	-2	-65	-26	-7	-1
		Spring	-116	-33	-10	-290	-115	-34	-6
		Summer	-207	-59	-18	-517	-205	-60	-10
		Autumn	-54	-15	-5	-135	-54	-16	-3

The table continues on next page.

Table 6. (Continued from previous page.)

Region	Component	Season	GWP, CO_2 equivalents (kt) 20 yrs	100 yrs	500 yrs	GTP, CO_2 equivalents (kt) 5 yrs	10 yrs	20 yrs	50 yrs
Offshore	BC (direct effect)	Winter	257	73	22	645	255	75	12
		Spring	616	175	53	1543	611	178	30
		Summer	592	168	51	1482	587	171	28
		Autumn	284	81	25	712	282	82	14
	BC (albedo effect)	Winter	448	127	39	1122	444	130	22
		Spring	1021	290	88	2556	1013	296	49
		Summer	988	281	85	2473	980	286	47
		Autumn	107	31	9	269	107	31	5
	OC	Winter	-5	-2	0	-13	-5	-2	0
		Spring	-16	-4	-1	-39	-16	-5	-1
		Summer	-25	-7	-2	-62	-25	-7	-1
		Autumn	-11	-3	-1	-27	-11	-3	-1
	SO_2	Winter	-20	-6	-2	-49	-19	-6	-1
		Spring	-65	-18	-6	-162	-64	-19	-3
		Summer	-108	-31	-9	-271	-107	-31	-5
		Autumn	-38	-11	-3	-95	-38	-11	-2
West	BC (direct effect)	Winter	352	100	30	882	349	102	17
		Spring	796	226	69	1992	789	230	38
		Summer	681	194	59	1706	676	197	33
		Autumn	334	95	29	837	332	97	16
	BC (albedo effect)	Winter	427	121	37	1069	424	124	21
		Spring	1044	296	90	2613	1035	302	50
		Summer	981	279	85	2457	973	284	47
		Autumn	99	28	9	248	98	29	5
	OC	Winter	-43	-12	-4	-108	-43	-13	-2
		Spring	-94	-27	-8	-236	-94	-27	-5
		Summer	-86	-24	-7	-215	-85	-25	-4
		Autumn	-44	-12	-4	-110	-43	-13	-2
	SO_2	Winter	-24	-7	-2	-60	-24	-7	-1
		Spring	-78	-22	-7	-195	-77	-23	-4
		Summer	-114	-32	-10	-286	-113	-33	-5
		Autumn	-49	-14	-4	-123	-49	-14	-2
Norway	BC (direct effect)	Annual	10068	2860	870	25208	9986	2915	484
	BC (albedo effect)	Annual	10800	3068	933	27040	10711	3127	519
	OC	Annual	-1199	-341	-104	-3003	-1190	-347	-58
	SO_2	Annual	-1318	-375	-114	-3297	-1306	-381	-63

4.2.2. Regional emission metrics

ARTP values have been calculated for emissions of BC, OC, and SO_2 and are presented in Figure 8 for time horizons of 20 and 100 years. The methodology is the same as in Collins et al. (2013), except that we give OC instead of POM (particulate organic matter). For BC, the calculations only include the direct effect. **The albedo effect is not included in these calculations as research is lacking in this**

field. The distribution of the temperature response from BC in each region will differ depending on whether the radiative forcing is from BC in the atmosphere or BC on snow/ice (the albedo effect). The methodology Shindell presents, and that is applied in Collins et al. (2013), takes only into consideration BC in the atmosphere. New model experiments with global climate models are needed to calculate RTP values for BC-albedo.

As for the ozone precursors (see Section 4.1.2), we see in Figure 8 that the response in each latitudinal band is relatively similar for emissions in the four different regions. As explained earlier, radiative forcing in the latitudinal bands used are relatively similar for the four emission regions in Norway because they are very close to each other compared to the resolution in the Shindell method. An exception is here the response of BC in the most northern latitudinal band (60°N-90°N), which show a larger dependency on emission region compared to the other response regions. In addition, the figure shows the sign is negative for this response region, thus, emissions of BC in Norway, especially from Northern Norway, apparently lead to a net cooling effect in the Arctic. The reason is most likely that Shindell focuses on global emissions, which would likely differ in characteristics compared to Norwegian emissions. If one applies the Shindell factors, an emission cut of BC in Norway would lead to a warming in the Arctic if we only focus on the direct effect in the atmosphere of BC. The link between positive radiative forcing and negative temperature response for BC in the Arctic (transported there from all sources globally) is shown in Figure 1d in Shindell and Faluvegi (2009) and has recently been confirmed by other studies (Flanner, 2013; Sand et al., 2013a), and is partly due to a reduction in meridional heat transport for BC high up in the atmosphere (approximately 230 hPa). This reduction in heat transport from the Tropics to the Arctic is caused by a reduced temperature difference between the Equator and North Pole since the BC particles lead to a warming of the upper layers in the troposphere in the Arctic. In addition, the BC particles in the atmosphere give a dimming at the surface. We would like to point out the large uncertainties and that only atmospheric BC is included in the estimates. The albedo effect (i.e. BC deposited on snow and ice), which in several cases is larger than the atmospheric direct effect with global emission metrics for Norwegian emissions (see Section 4.2.1), gives probably a warming in the Arctic independent of whether the emissions occur inside or outside of the Arctic (Sand et al., 2013b). Emissions at higher latitudes result in an increase in BC relatively low in the atmosphere, which in turn increase the probability of deposition on snow and ice surfaces and, thus, give a warming effect (Flanner, 2013). Hence, the net impact of BC emissions in Norway is most likely a warming of the Arctic, even though the Shindell method, which does not consider the albedo effect, shows the opposite (Figure 8). A new study by Sand et al. (2013b) shows that emissions from both the mid-latitudes (28-60 °N) and Arctic (60-90 °N) give an increased temperature at the surface in the Arctic when the albedo effect is included. Emissions in the Arctic lead to a warming at the surface in the Arctic five times as strong (per kg emissions) than emissions from mid-latitudes. We would like to point out the large uncertainty for the effect of BC emissions, both in terms of radiative forcing and temperature response.

For the scattering aerosols, OC and sulphate, the response is negative in all latitudinal bands (Figure 8). Hence, emissions of OC and sulphate from all the four Norwegian regions lead to a cooling over the entire globe. The response is strongest in the Arctic latitudinal band, partly because the radiative forcing is strongest here, but also due to the strong correlation between radiative forcing in the Northern mid-latitudinal band (28°N-60°N) and the temperature response in the Arctic. The short lifetime of the aerosols causes the radiative forcing, and the temperature response as well, to be

largest in the latitudinal bands that are closest to the location of the emissions, while the temperature response for Norwegian emissions of ozone precursors is somewhat more spread over the globe due to the long term effects (methane and ozone "primary mode" – see Section 3.3). For the aerosols, the distribution between the different latitudinal bands for the temperature response is identical for all time horizons, but with differences in the total size, as illustrated for time horizons of 20 and 100 years in Figure 8. The uncertainties for the regional temperature responses of the aerosols are large, as for ARTP for the ozone precursors, thus, these results should only be interpreted as an indication of how the distribution may look like for emissions in Norway.

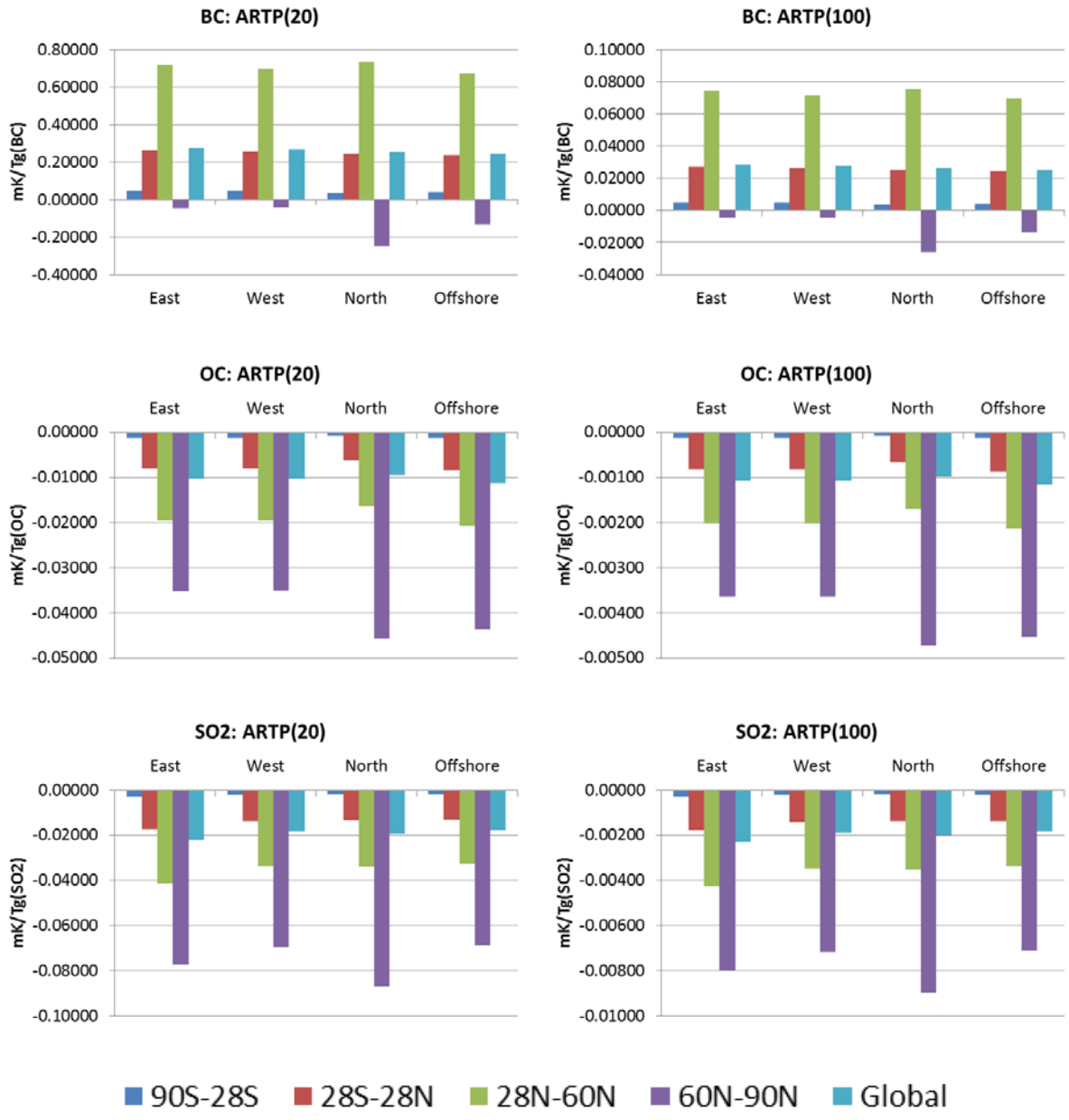

Figure 8. ARTP values for time horizons of 20 years (left) and 100 years (right) for emissions of BC, OC, and SO_2 in the four Norwegian regions (units are mK/Tg(BC), mK/Tg(OC), and mK/Tg(SO_2), respectively). The columns show the temperature response in four different latitudinal bands (90°S-28°S, 28°S-28°N, 28°N-60°N, and 60°N-90°N) and globally.

4.2.3. Uncertainties

Aerosols have both direct and indirect effects. We name and numerate the various processes according to AR4 IPCC language. While the direct effect is caused by scattering and/or absorption of incoming solar radiation, the indirect effects change the microphysical and radiation properties of clouds, as well as amount of clouds and lifetime of clouds. The semi-direct effect includes warming of clouds from the aerosols, which leads to evaporation (burn-off) of clouds. Aerosols will also affect ice clouds and clouds that consist of a mix of ice crystals and water droplets (mix phase). The indirect effect is often divided into the "cloud albedo effect" (first indirect effect) and "cloud lifetime effect" (second indirect effect). To separate the different contributions to the indirect effect is difficult for the different aerosol types. The estimate given as the most likely value in Forster et al. (2007) indicates that the indirect effect is larger than the direct effect, and a factor of 1.5-2 can be applied to give a rough estimate of the indirect effect relative to the direct effect, but the uncertainty here is large.

The uncertainty in the direct effect of the anthropogenic radiative forcing of aerosols in AR4 is estimated to ±80%, with variations between the aerosol types. For instance, the radiative forcing of sulphate particles has lower uncertainty (±50%) than the radiative forcing for fossil BC (±75%) and OC (±100%). In a new study by Myhre et al. (2013), 16 detailed global aerosol models were included to estimate the direct aerosol effect due to anthropogenic emissions. They conclude that the differences between the models are large, for instance, the relative standard deviation for the radiative forcing for fossil BC is larger than 40%, but the uncertainty in the total direct aerosol effect is smaller than the sum of the direct aerosol effect of the individual aerosol components.

The indirect effects of aerosols have significantly larger uncertainties than the direct effects. In AR4, the second indirect effect is described in Section 7.5.2, but the uncertainty is so large that no estimate of its size has been given, just that this effect is negative (cooling). The first indirect effect is somewhat less uncertain, but still the uncertainty is very large; +160/-57% compared to the best estimate for the globally averaged radiative forcing of 0.70 W m^{-2}.

4.3. Methane (CH_4) and hydrofluorcarbons (HFC)

4.3.1. Global emission metrics

Global GWP and GTP values based on AR4 (Forster et al., 2007) for various components are presented in Table 7 for time horizons of 20, 100, and 500 years for GWP, and 5, 10, 20, and 50 years for GTP. Results for all time horizons between 0 and 500 years, as well as GWP and GTP values for a modified version of constant emissions, are available in Annex 1 («GWP_GTP_pulse_scenario_ENGLISH.xlsx»). Updated GWP and GTP values for HFCs are given in Table 8 (Hodnebrog et al., 2013).

Table 7. GWP and GTP values for different time horizons (for pulse emissions) for CH_4 and some HFCs. These values are based on AR4 (Forster et al., 2007).

	GWP			GTP			
	20 yrs	100 yrs	500 yrs	5 yrs	10 yrs	20 yrs	50 yrs
CH_4	72.1	25.2	7.7	100.7	86.5	57.3	12.2
HFC-23	12003	14784	12242	10454	11354	12779	15565
HFC-32	2334	675	205	4904	3180	1263	142
HFC-125	6346	3504	1100	6785	6700	6044	3367
HFC-134	3393	1101	335	5204	4231	2501	407
HFC-134a	3825	1428	435	5037	4470	3176	819
HFC-143	1235	352	107	2984	1682	563	67
HFC-143a	5886	4472	1592	5706	5903	5927	4809
HFC-152a	437	124	38	1239	514	148	22
HFC-227ea	5307	3222	1035	5491	5509	5153	3257

Table 8. GWP and GTP values for different time horizons (for pulse emissions) for CH_4 and some HFCs. These values are based on a new study by Hodnebrog et al. (2013).

	GWP			GTP			
	20 yrs	100 yrs	500 yrs	5 yrs	10 yrs	20 yrs	50 yrs
HFC-23	10827	12398	8721	9298	10259	11524	12959
HFC-32	2435	677	193	4879	3299	1362	145
HFC-125	6094	3169	930	6427	6445	5797	2977
HFC-134	3580	1116	318	5359	4450	2656	412
HFC-134a	3710	1301	371	4868	4362	3053	703
HFC-143	1202	328	94	2848	1634	549	62
HFC-143a	6941	4804	1556	6686	7001	6957	5061
HFC-152a	506	138	39	1405	601	174	24
HFC-227ea	5358	3348	1034	5313	5488	5283	3436

4.3.2. Uncertainties

Joos et al. (2013) have estimated an uncertainty for the Absolute Global Warming Potential (AGWP) for the reference gas CO_2 to ±18%, ±26%, and ±30% for time horizons of 20, 100, and 500 years, respectively. The uncertainty in GWP for CH_4 is discussed in Aamaas et al. (2013) and estimated to approximately 66% (for 5-95% confidence interval) for a time horizon of 100 years. For the HFCs, the uncertainties are dependent on a number of factors, as described in Hodnebrog et al. (2013), especially the lifetime of the component. For HFC gases with lifetimes longer than 5 years, the total uncertainty in the radiative forcing is estimated to ~13%, while increasing to ~23% for HFC -gases with shorter lifetimes than 5 years. If one includes the uncertainty in AGWP of CO_2, as described previously, and uncertainty in lifetime, the total uncertainty in GWP (for 5-95% (90%) confidence interval) is for instance for HFC-134a approximately ±24%, ±34%, and ±37% for time horizons of 20, 100, and 500 years, respectively (Hodnebrog et al., 2013).

As discussed in Section 4.1.4, the uncertainty increases as one moved from the emission metric GWP to GTP since the emission metric must then include a function that describes the temperature response from a radiative forcing. A study by Olivié and Peters (2013) found increasing uncertainty in GTP, as a result of increasing uncertainty in the temperature response function with increasing time horizons and lower uncertainty for longer lifetimes. For methane, they found an uncertainty in GTP of -16/+26% for a time horizon of 20 years, increasing to -76/+68% for a time horizon of 100 years. In comparison, the uncertainty in GWP for a time horizon of 20 years is -9/+16% and -14/+22% for a time horizon of 100 years. Components with shorter lifetimes have even larger uncertainty intervals in GTP.

Glossary

- AGTP/GTP: Absolute Global Temperature change Potential is the change in global surface temperature at a given point in time after a pulse emission occurred. The unit for AGTP is °C per kg emitted. The emission metric is called GTP (Global Temperature change Potential) when normalized to the reference gas, CO_2.
- AGWP/GWP: Absolute Global Warming Potential is the cumulative of the radiative forcing up to a given point in time. The unit for AGWP is W/m^2*yr per kg emitted. The emission metric is called GWP (Global Warming Potential) when normalized to the reference gas CO_2. GWP with a time horizon of 100 years is often used, for instance adopted by the Kyoto Protocol.
- Perturbation: An increase or decrease relative to a given reference level, e.g., the global emissions.
- Pulse emissions: In this report, emissions occurring during the first year, followed by no emissions. Emission metrics are normally based on pulse emissions.
- Radiative forcing: A change (for instance due to a change in the concentration of CO_2) in net (down minus up) irradiance (solar radiation and longwave radiation, in W/m^2) at the tropopause AFTER the stratospheric temperature has adjusted to a new radiation equilibrium, while the temperature at the surface and in the troposphere is kept unchanged at initial values. In other words: Energy change per unit of area on Earth measured at the top of the atmosphere.
- Emission metric: The two most common emission metrics are GWP and GTP. The emission metrics makes climate impacts of different types comparable. The climate impact is only comparable for the chosen emission metric and its impact parameter and chosen time horizon.

References

Aamaas, B., Peters, G. P., Fuglestvedt, J. S., and Berntsen, T. K.: How to compare different short-lived climate forcers – a review of emission metrics, A CICERO report to Klif, July 2012, 2012.

Aamaas, B., Peters, G. P., and Fuglestvedt, J. S.: Simple emission metrics for climate impacts, Earth Syst. Dynam., 4, 145-170, 10.5194/esd-4-145-2013, 2013.

Bauer, S. E., Koch, D., Unger, N., Metzger, S. M., Shindell, D. T., and Streets, D. G.: Nitrate aerosols today and in 2030: a global simulation including aerosols and tropospheric ozone, Atmospheric Chemistry and Physics, 7, 19, 5043-5059, 2007.

Berglen, T. F., Berntsen, T. K., Isaksen, I. S. A., and Sundet, J. K.: A global model of the coupled sulfur/oxidant chemistry in the troposphere: The sulfur cycle, J. Geophys. Res.-Atmos., 109, D19310, 10.1029/2003jd003948, 2004.

Berntsen, T., Fuglestvedt, J., Myhre, G., Stordal, F., and Berglen, T. F.: Abatement of greenhouse gases: Does location matter?, Climatic Change, 74, 4, 377-411, 10.1007/s10584-006-0433-4, 2006.

Berntsen, T., and Fuglestvedt, J.: Global temperature responses to current emissions from the transport sectors, Proc. Natl. Acad. Sci. U. S. A., 105, 49, 19154-19159, 10.1073/pnas.0804844105, 2008.

Berntsen, T. K., and Isaksen, I. S. A.: A global three-dimensional chemical transport model for the troposphere .1. Model description and CO and ozone results, J. Geophys. Res.-Atmos., 102, D17, 21239-21280, 10.1029/97jd01140, 1997.

Berntsen, T. K., Fuglestvedt, J. S., Joshi, M. M., Shine, K. P., Stuber, N., Ponater, M., Sausen, R., Hauglustaine, D. A., and Li, L.: Response of climate to regional emissions of ozone precursors: sensitivities and warming potentials, Tellus Ser. B-Chem. Phys. Meteorol., 57, 4, 283-304, 2005.

Boer, G. J., and Yu, B.: Climate sensitivity and response, Clim. Dyn., 20, 4, 415-429, 10.1007/s00382-002-0283-3, 2003.

Bond, T. C., Zarzycki, C., Flanner, M. G., and Koch, D. M.: Quantifying immediate radiative forcing by black carbon and organic matter with the Specific Forcing Pulse, Atmos. Chem. Phys., 11, 4, 1505-1525, 10.5194/acp-11-1505-2011, 2011.

Bond, T. C., Doherty, S. J., Fahey, D. W., Forster, P. M., Berntsen, T., DeAngelo, B. J., Flanner, M. G., Ghan, S., Kärcher, B., Koch, D., Kinne, S., Kondo, Y., Quinn, P. K., Sarofim, M. C., Schultz, M. G., Schulz, M., Venkataraman, C., Zhang, H., Zhang, S., Bellouin, N., Guttikunda, S. K., Hopke, P. K., Jacobson, M. Z., Kaiser, J. W., Klimont, Z., Lohmann, U., Schwarz, J. P., Shindell, D., Storelvmo, T., Warren, S. G., and Zender, C. S.: Bounding the role of black carbon in the climate system: A scientific assessment, Journal of Geophysical Research: Atmospheres, 10.1002/jgrd.50171, 2013.

Colette, A., Granier, C., Hodnebrog, O., Jakobs, H., Maurizi, A., Nyiri, A., Bessagnet, B., D'Angiola, A., D'Isidoro, M., Gauss, M., Meleux, F., Memmesheimer, M., Mieville, A., Rouil, L., Russo, F., Solberg, S., Stordal, F., and Tampieri, F.: Air quality trends in Europe over the past decade: a first multi- model assessment, Atmospheric Chemistry and Physics, 11, 22, 11657-11678, 10.5194/acp-11-11657-2011, 2011.

Collins, W. J., Derwent, R. G., Johnson, C. E., and Stevenson, D. S.: The oxidation of organic compounds in the troposphere and their global warming potentials, Climatic Change, 52, 4, 453-479, 10.1023/a:1014221225434, 2002.

Collins, W. J., Sitch, S., and Boucher, O.: How vegetation impacts affect climate metrics for ozone precursors, J. Geophys. Res.-Atmos., 115, 10.1029/2010jd014187, 2010.

Collins, W. J., Fry, M. M., Yu, H., Fuglestvedt, J. S., Shindell, D. T., and West, J. J.: Global and regional temperature-change potentials for near-term climate forcers, Atmos. Chem. Phys., 13, 5, 2471-2485, 10.5194/acp-13-2471-2013, 2013.

Derwent, R. G., Collins, W. J., Johnson, C. E., and Stevenson, D. S.: Transient behaviour of tropospheric ozone precursors in a global 3-D CTM and their indirect greenhouse effects, Climatic Change, 49, 4, 463-487, 10.1023/a:1010648913655, 2001.

Flanner, M. G.: Arctic climate sensitivity to local black carbon, Journal of Geophysical Research: Atmospheres, n/a-n/a, 10.1002/jgrd.50176, 2013.

Forster, P. M., Ramaswamy, V., Artaxo, P., Berntsen, T., Betts, R., Fahey, D. W., Haywood, J., Lean, J., Lowe, D. C., Myhre, G., Nganga, J., Prinn, R., Raga, G., Schulz, M., and Van Dorland, R.: Changes in Atmospheric Constituents and in Radiative Forcing, In: Climate Change 2007: The Physical Science Basis. Contribution of Working Group I to the Fourth Assessment Report of the Intergovernmental Panel on Climate Change eds. Solomon, S., D. Qin, M. Manning, Z. Chen, M. Marquis et al. , Cambridge, United Kingdom and New York, NY, USA, 129-234, 2007.

Fry, M. M., Naik, V., West, J. J., Schwarzkopf, M. D., Fiore, A. M., Collins, W. J., Dentener, F. J., Shindell, D. T., Atherton, C., Bergmann, D., Duncan, B. N., Hess, P., MacKenzie, I. A., Marmer, E., Schultz, M. G., Szopa, S., Wild, O., and Zeng, G.: The influence of ozone precursor emissions from four world regions on tropospheric composition and radiative climate forcing, J. Geophys. Res.-Atmos., 117, 10.1029/2011jd017134, 2012.

Fuglestvedt, J. S., Shine, K. P., Berntsen, T., Cook, J., Lee, D. S., Stenke, A., Skeie, R. B., Velders, G. J. M., and Waitz, I. A.: Transport impacts on atmosphere and climate: Metrics, Atmospheric Environment, 44, 37, 4648-4677, 10.1016/j.atmosenv.2009.04.044, 2010.

Fujino, J., Nair, R., Kainuma, M., Masui, T., and Matsuoka, Y.: Multi-gas mitigation analysis on stabilization scenarios using aim global model, Energy Journal, 343-353, 2006.

Grini, A., Myhre, G., Sundet, J. K., and Isaksen, I. S. A.: Modeling the annual cycle of sea salt in the global 3D model Oslo CTM2: Concentrations, fluxes, and radiative impact, J. Clim., 15, 13, 1717-1730, 10.1175/1520-0442(2002)015<1717:mtacos>2.0.co;2, 2002.

Hodnebrog, Ø., Etminan, M., Fuglestvedt, J. S., Marston, G., Myhre, G., Nielsen, C. J., Shine, K. P., and Wallington, T. J.: Global Warming Potentials and Radiative Efficiencies of Halocarbons and Related Compounds: A Comprehensive Review, Rev. Geophys., 51, 2, 300-378, 10.1002/rog.20013, 2013.

IPCC: Climate Change 2001: The Scientific Basis. Contribution of Working Group I to the Third Assessment Report of the Intergovernmental Panel on Climate Change, Cambridge University Press, Cambridge, United Kingdom and New York, NY, USA., 881, 2001.

Jacob, D. J.: Introduction to Atmospheric Chemistry, Princeton University Press, 1999.

Joos, F., Roth, R., Fuglestvedt, J. S., Peters, G. P., Enting, I. G., von Bloh, W., Brovkin, V., Burke, E. J., Eby, M., Edwards, N. R., Friedrich, T., Frölicher, T. L., Halloran, P. R., Holden, P. B., Jones, C., Kleinen, T., Mackenzie, F., Matsumoto, K., Meinshausen, M., Plattner, G. K., Reisinger, A., Segschneider, J., Shaffer, G., Steinacher, M., Strassmann, K., Tanaka, K., Timmermann, A., and Weaver, A. J.: Carbon dioxide and climate impulse response functions for the computation of greenhouse gas metrics: a multi-model analysis, Atmos. Chem. Phys., 13, 2793-2825, 10.5194/acp-13-2793-2013, 2013.

Myhre, G., Karlsdottir, S., Isaksen, I. S. A., and Stordal, F.: Radiative forcing due to changes in tropospheric ozone in the period 1980 to 1996, J. Geophys. Res.-Atmos., 105, D23, 28935-28942, 2000.

Myhre, G., Grini, A., and Metzger, S.: Modelling of nitrate and ammonium-containing aerosols in presence of sea salt, Atmos. Chem. Phys., 6, 12, 4809-4821, 10.5194/acp-6-4809-2006, 2006.

Myhre, G., Bellouin, N., Berglen, T. F., Berntsen, T. K., Boucher, O., Grini, A., Isaksen, I. S. A., Johnsrud, M., Mishchenko, M. I., Stordal, F., and Tanre, D.: Comparison of the radiative properties and direct radiative effect of aerosols from a global aerosol model and remote sensing data over ocean, Tellus Ser. B-Chem. Phys. Meteorol., 59, 1, 115-129, 10.1111/j.1600-0889.2006.00226.x, 2007a.

Myhre, G., Nilsen, J. S., Gulstad, L., Shine, K. P., Rognerud, B., and Isaksen, I. S. A.: Radiative forcing due to stratospheric water vapour from CH4 oxidation, Geophys. Res. Lett., 34, L01807, 10.1029/2006gl027472, 2007b.

Myhre, G., Samset, B. H., Schulz, M., Balkanski, Y., Bauer, S., Berntsen, T. K., Bian, H., Bellouin, N., Chin, M., Diehl, T., Easter, R. C., Feichter, J., Ghan, S. J., Hauglustaine, D., Iversen, T., Kinne, S., Kirkevåg, A., Lamarque, J. F., Lin, G., Liu, X., Lund, M. T., Luo, G., Ma, X., van Noije, T., Penner, J. E., Rasch, P. J., Ruiz, A., Seland, Ø., Skeie, R. B., Stier, P., Takemura, T., Tsigaridis, K., Wang, P., Wang, Z., Xu, L., Yu, H., Yu, F., Yoon, J. H., Zhang, K., Zhang, H., and Zhou, C.: Radiative forcing of the direct aerosol effect from AeroCom Phase II simulations, Atmos. Chem. Phys., 13, 4, 1853-1877, 10.5194/acp-13-1853-2013, 2013.

Olivié, D. J. L., and Peters, G. P.: Variation in emission metrics due to variation in CO2 and temperature impulse response functions, Earth Syst. Dynam., 4, 2, 267-286, 10.5194/esd-4-267-2013, 2013.

Rypdal, K., Rive, N., Berntsen, T. K., Klimont, Z., Mideksa, T. K., Myhre, G., and Skeie, R. B.: Costs and global impacts of black carbon abatement strategies, Tellus Ser. B-Chem. Phys. Meteorol., 61, 4, 625-641, 10.1111/j.1600-0889.2009.00430.x, 2009.

Samset, B. H., and Myhre, G.: Vertical dependence of black carbon, sulphate and biomass burning aerosol radiative forcing, Geophys. Res. Lett., 38, 10.1029/2011gl049697, 2011.

Sand, M., Berntsen, T. K., Kay, J. E., Lamarque, J. F., Seland, Ø., and Kirkevåg, A.: The Arctic response to remote and local forcing of black carbon, Atmos. Chem. Phys., 13, 1, 211-224, 10.5194/acp-13-211-2013, 2013a.

Sand, M., Berntsen, T. K., Seland, Ø., and Kristjánsson, J. E.: Arctic surface temperature change to emissions of black carbon within Arctic or mid-latitudes, Journal of Geophysical Research: Atmospheres, 118, 7788–7798, 10.1002/jgrd.50613, 2013b.

Shindell, D., and Faluvegi, G.: Climate response to regional radiative forcing during the twentieth century, Nature Geoscience, 2, 4, 294-300, 10.1038/ngeo473, 2009.

Shindell, D., and Faluvegi, G.: The net climate impact of coal-fired power plant emissions, Atmospheric Chemistry and Physics, 10, 7, 3247-3260, 2010.

Shindell, D. T., Faluvegi, G., Koch, D. M., Schmidt, G. A., Unger, N., and Bauer, S. E.: Improved Attribution of Climate Forcing to Emissions, Science, 326, 5953, 716-718, 10.1126/science.1174760, 2009.

Shindell, D. T.: Evaluation of the absolute regional temperature potential, Atmos. Chem. Phys. Discuss., 12, 6, 13813-13825, 10.5194/acpd-12-13813-2012, 2012.

Sitch, S., Cox, P. M., Collins, W. J., and Huntingford, C.: Indirect radiative forcing of climate change through ozone effects on the land-carbon sink, Nature, 448, 7155, 791-U794, 10.1038/nature06059, 2007.

Skeie, R. B., Berntsen, T. K., Myhre, G., Tanaka, K., Kvalevåg, M. M., and Hoyle, C. R.: Anthropogenic radiative forcing time series from pre-industrial times until 2010, Atmos. Chem. Phys., 11, 22, 11827-11857, 10.5194/acp-11-11827-2011, 2011.

Streets, D. G., Bond, T. C., Carmichael, G. R., Fernandes, S. D., Fu, Q., He, D., Klimont, Z., Nelson, S. M., Tsai, N. Y., Wang, M. Q., Woo, J. H., and Yarber, K. F.: An inventory of gaseous and primary aerosol emissions in Asia in the year 2000, J. Geophys. Res.-Atmos., 108, D21, 10.1029/2002jd003093, 2003.

Søvde, O. A., Gauss, M., Smyshlyaev, S. P., and Isaksen, I. S. A.: Evaluation of the chemical transport model Oslo CTM2 with focus on arctic winter ozone depletion, J. Geophys. Res.-Atmos., 113, D09304, 10.1029/2007jd009240, 2008.

van der Werf, G. R., Randerson, J. T., Giglio, L., Collatz, G. J., Mu, M., Kasibhatla, P. S., Morton, D. C., DeFries, R. S., Jin, Y., and van Leeuwen, T. T.: Global fire emissions and the contribution of deforestation, savanna, forest, agricultural, and peat fires (1997–2009), Atmos. Chem. Phys., 10, 23, 11707-11735, 10.5194/acp-10-11707-2010, 2010.

van Vuuren, D. P., Edmonds, J., Kainuma, M., Riahi, K., Thomson, A., Hibbard, K., Hurtt, G. C., Kram, T., Krey, V., Lamarque, J. F., Masui, T., Meinshausen, M., Nakicenovic, N., Smith, S. J., and Rose, S. K.: The representative concentration pathways: an overview, Climatic Change, 109, 1-2, 5-31, 10.1007/s10584-011-0148-z, 2011.

Wild, O., Prather, M. J., and Akimoto, H.: Indirect long-term global radiative cooling from NOx emissions, Geophys. Res. Lett., 28, 9, 1719-1722, 10.1029/2000gl012573, 2001.

Zhang, R. Y., Tie, X. X., and Bond, D. W.: Impacts of anthropogenic and natural NOx sources over the US on tropospheric chemistry, Proc. Natl. Acad. Sci. U. S. A., 100, 4, 1505-1509, 10.1073/pnas.252763799, 2003.

Ødemark, K., Dalsøren, S. B., Samset, B. H., Berntsen, T. K., Fuglestvedt, J. S., and Myhre, G.: Short-lived climate forcers from current shipping and petroleum activities in the Arctic, Atmospheric Chemistry and Physics, 12, 4, 1979-1993, 10.5194/acp-12-1979-2012, 2012.